

1 **Multidrug resistance protein 4 (MRP4/ABCC4) is overexpressed in clear cell renal cell**
2 **carcinoma (ccRCC) and is essential to regulate cell proliferation**

3
4
5
6
7
8
9
10 5 Juan Pablo Melana Colavita¹, Juan Santiago Todaro¹, Maximiliano de Sousa², María May²,
11 6 Natalia Gomez², Agustin Yaneff², Nicolas Di Siervi², María Victoria Aguirre¹, Carlos Guijas³,
12 7 Leandro Ferrini²; Carlos Davio², Juan Pablo Rodríguez^{1,#}.

- 13
14
15
16
17
18
19
20 9 1. Laboratorio de Investigaciones Bioquímicas de la Facultad de Medicina (LIBIM).
21 Instituto de Química Básica y Aplicada del NEA, (IQUIBA NEA-UNNE- CONICET),
22 10 Facultad de Medicina, Universidad Nacional del Nordeste, 3400 Corrientes,
23 11 Argentina.
24
25
26
27
28
29
30 13 2. Instituto de Investigaciones Farmacológicas (ININFA-UBA-CONICET), Facultad
31 de Farmacia y Bioquímica, Universidad de Buenos Aires, 1000 Buenos Aires,
32 14 Argentina.
33 15
34
35
36
37
38 16 3. Instituto de Biología y Genética Molecular, Consejo Superior de Investigaciones
39 Científicas (CSIC), Universidad de Valladolid, 47003 Valladolid, España.
40 17
41
42
43
44
45
46

47 20 **# Corresponding author:** Juan Pablo Rodríguez, Ph.D.

48
49
50 21 Laboratorio de Investigaciones Bioquímicas de la Facultad de Medicina (LIBIM-IQUIBA-
51 UNNE-CONICET), Facultad de Medicina, Universidad Nacional del Nordeste, 3400
52 22 Corrientes, Argentina. rodriguezcasco@med.unne.edu.ar
53
54
55
56
57
58
59
60
61
62
63
64
65

26 **Abstract**

1
2 27 Kidney cancer accounts for 2.5% of all cancers, with an annual global incidence of almost
3
4 28 300,000 cases leading to 111,000 deaths. Approximately 85% of kidney tumors are renal
5
6
7 29 cell carcinoma (RCC) and their major histologic subtype is clear cell renal cell carcinoma
8
9
10 30 (ccRCC). Although new therapeutic treatments are being designed and applied based on
11
12 31 the combination of tyrosine kinase inhibitors and immunotherapy, no major impact on the
13
14 32 mortality has been reported so far.

16
17 33 MRP4 is a pump efflux that transporters multiple endogenous and exogenous substances.
18
19
20 34 Recently it has been associated with tumoral persistence and cell proliferation in several
21
22 35 types of cancer including pancreas, lung, ovary, colon, osteosarcoma, etc.

24
25 36 Herein, we demonstrate for the first time, that MRP4 is overexpressed in ccRCC tumors,
26
27 37 compared to control renal tissues. In addition, using cell culture models, we observed that
28
29
30 38 MRP4 pharmacological inhibition produces an imbalance in cAMP metabolism, induces cell
31
32 39 arrest, changes in lipid composition, increase in cytoplasmic lipid droplets and finally
33
34
35 40 apoptosis.

36
37
38 41 These data provide solid evidence for the future evaluation of MRP4 as a possible new
39
40
41 42 therapeutic target in ccRCC.

42
43 43

44
45 44

46
47 45 **KEY WORDS:** cAMP; MRP4; lipidomics, renal carcinoma.

48
49 46

50
51 47

52
53 48

54
55 49

56
57 50

58
59
60
61
62
63
64
65

51 **1. Introduction**

1
2 52 Renal cell carcinoma (RCC) is the most common type of adult kidney malignant
3
4 53 tumor. Clear cell Renal Cell Carcinoma (ccRCC) is the predominant histological subtype
5
6
7 54 of RCC (75–80 %) and is usually associated with severe prognosis and high mortality [1].
8
9
10 55 About 30% of ccRCC are diagnosed at the metastatic stage and it is treated by
11
12 56 nephrectomy, however a third of the patients after resection of the tumor will have a
13
14
15 57 recurrence [2].
16

17 58 Conventional systemic therapeutic treatments on advanced ccRCC, like cytotoxic
18
19
20 59 drugs and radiotherapy resulted largely ineffective and did not improve patient survival
21
22 60 [3]. Currently, recommended first-line targeted therapy options are single-agent
23
24
25 61 tyrosine kinase inhibitors (TKIs) including pazopanib, sunitinib, axitinib and cabozantinib,
26
27
28 62 or temsirolimus, which targets mTOR. In addition, immune checkpoint inhibitors were
29
30
31 63 introduced, with encouraging results. Nevertheless, RCC incidence has been stable and
32
33 64 death rates have been falling only 0.9% each year from 2007 through 2016 [4].
34

35 65 Recently it has been described the existence of drug/metabolites efflux proteins
36
37
38 66 pumps, on the basolateral or apical side of cells, that might be involved in the
39
40
41 67 persistence of tumors modulating levels of physiological mediators. [5–7].
42

43 68 Among them, multidrug resistance protein 4 (MRP4) is member of ATP-binding
44
45
46 69 cassette (ABC) transporters (C4 subtype), responsible for ATP-driven transmembranous
47
48
49 70 transport of substrates [8]. MRP4 (MOAT-B; multi- specific organic anion transporter) is
50
51
52 71 a lipophilic anion efflux pump that was categorized as a short MRP, and has similar
53
54
55 72 membrane topologies as MRP5, 8, and 9 [9]. To date, nine MRPs have been identified
56
57
58 73 and are able to transport a wide variety of endogenous and xenobiotic organic anions
59
60
61 74 out of the cell [10,11]. Each MRP has its own membrane location, tissue distribution,
62
63
64
65

75 and substrate specificity. Especially, MRP4 has a particular broad substrate specificity,
1 76 encompassing cyclic nucleotides (especially cAMP), ADP, eicosanoids, urate, steroid
2
3
4 77 hormones, folate, and bile acids among others endogenous substrates and several
5
6
7 78 antiviral, antibiotic, cardiovascular, cytotoxic (methotrexate, 6-thioguanine, 6-
8
9
10 79 mercaptopurine, topotecan) exogenous drugs [12,13]. Additionally, there are other
11
12 80 carriers related to MRPs, such as OATP4C1 that has a reverse transport flow of
13
14
15 81 metabolites, compared to MRP4 [14].

16
17 82 It has been reported in different cancer types, that MRP4 dysregulation is
18
19 83 associated with cell proliferation and malignancy [15]. Moreover, it was observed in
20
21
22 84 neuroblastoma that high levels of MRP4 expression were significantly associated with
23
24
25 85 poor clinical prognosis, and it was proposed as a prognostic biomarker and therapeutic
26
27 86 target [8,16]. Although historically the role of MRPs proteins in cancer was associated
28
29
30 87 with chemotherapy resistance, nowadays, there are many additional experimental
31
32 88 evidences that relate poor prognosis with endobiotics transport, cAMP and
33
34
35 89 prostaglandins, which are vital for tumor progression and malignancy [17–19].

36
37
38 90 On the other hand, the cAMP balance is critical for the lipids metabolism and
39
40 91 formation of lipid droplets in cancer [20], a particular phenotypic characteristic of ccRCC
41
42
43 92 [21].

44
45 93 There are no previous reports describing the MRP4 expression and its role in ccRCC
46
47
48 94 related to cAMP metabolism. So it is likely that MRP4 is particularly involved in tumor
49
50
51 95 characteristics and be responsible, at least in part, for the clinically observed
52
53 96 chemoresistance [3].

54
55
56 97 The objective of this work was to evaluate the expression and functionality of MRP4
57
58 98 in ccRCC and its association with malignancy, in order to postulate it as a potential
59
60
61
62
63
64
65

99 biomarker of prognosis and / or pharmacological target for the development of more
100 effective therapeutic strategies.

101

102 **2. Materials and methods**

103 *2.1. In Silico Analysis of MRP4/ABCC4 expression in ccRCC patients*

104 In order to determine the prognostic value of MRP4/ABCC4 expression in patients
105 diagnosed with ccRCC, we first evaluated its expression levels, using related studies
106 hosted in Array Express. Through a script, the sequencing platform's ID used in each
107 study was retrieved from NCBI's site, then the platform's data table containing the
108 probe's ID for ABCC4 were downloaded. The expression matrix file for each study
109 was downloaded through NCBI's ftp site. Then ABCC4's expression levels for each
110 sample was extracted along with the sample's description. This was used to
111 evaluate if there was significant differential expression among sample types (ccRCC
112 vs adjacent non-tumoral renal cells)[22,23].

113 *2.2. Patients and sampling procedures*

114 Surgical specimens were obtained from 32 patients with ccRCC. Patients were
115 treated by radical nephrectomy at the Urology Unit of the J.R. Vidal Hospital
116 (Corrientes, Argentina) between 2013 and 2018. Surgically removed ccRCC and
117 counterpart normal tissues (tissue sections away from the tumor in the same
118 kidney) were collected from specimens, transported aseptically to the laboratory,
119 and quickly frozen at -80°C. Specimens were fixed for histopathology and
120 immunohistochemistry procedures.

121 The design and methods of this research have been approved by the Bioethics
122 Committee of the School of Medicine of the Northeastern National University and

123 by the Department of Medical Research of the J.R. Vidal Hospital from Corrientes,
124 Argentina.

125 2.3. *RT-qPCR*

126 MRP4 messenger RNA (mRNA) expression was extracted using the TRIzol reagent
127 method (Invitrogen) and purified using Ambion® TURBO DNA-free™ according to
128 the manufacturer's protocol. First-strand cDNA was obtained by using the MMLV-
129 RT (Promega) from 2 µg of RNA. qPCRs were then performed using specific primers
130 for MRP4 as follows: 5'-GGACAAAGACAACACTGGTGTGCC-3' (forward), 5'-
131 AATGGTTAGCACGGTGCAGTGG-3' (reverse) with a product of 156 bp. GAPDH: 5'-
132 ATGGGGAAGGTGAAGGTCG-3' (forward); 5'- GGGGTCATTGATGGCAACAATA-3'
133 (reverse) with a product of 108 bp or β-Actin: 5'-CATGTACGTTGCTATCCAGGC-3'
134 (forward); 5'- CTCCTTAATGTACGCACGAT-3' (reverse) with a product of 250 bp
135 were used as housekeeping genes and no differences were overserved between
136 them. All primers were tested for specificity using the Blast program available at the
137 National Center for Biotechnology Information web site. Cycling conditions were as
138 follows: 1 cycle at 95 °C for 10min, 35 cycles at 95°C for 30 s, 58°C for 45 s, 72 °C for
139 1 min, and a final extension at 72 °C for 10 min.

140 2.4. *Western blot analysis*

141 Expression of MRP4 was determined by immunoblotting using total cell lysates.
142 Samples from ccRCC patients and a distal section of renal normal tissue of each
143 patient were homogenized and lysed in an ice-cold buffer [10 mM HEPES pH 7.4, 10
144 mM KCl, 1.5 mM MgCl₂, 0.5 mM dithiothreitol, 0.1% IGEPAL (Sigma Co, MO, USA)],
145 supplemented with a protease inhibitor cocktail.

1
2
3
4
5
6
7
8
9
10
11
12
13
14
15
16
17
18
19
20
21
22
23
24
25
26
27
28
29
30
31
32
33
34
35
36
37
38
39
40
41
42
43
44
45
46
47
48
49
50
51
52
53
54
55
56
57
58
59
60
61
62
63
64
65

146 Total proteins (50 µg) were then separated by 8% SDS-PAGE and blotted on
147 nitrocellulose membranes (Bio-Rad, CA, USA). Membranes were then treated with
148 1:500 dilutions of primary antibodies purchased at Santa Cruz® biotechnologies and
149 after that probed with the corresponding antibodies followed by HRP-conjugated
150 secondary antibodies in TBS solution. β-Actin was used as a load control. The
151 immunoblots were visualized using enhanced luminescence (ECL, BIO-RAD).
152 Densitometry was performed on scanned images using ImageJ software (NIH; Ver
153 1.52a), and values were normalized for the corresponding controls of each
154 experiment. All experiments were performed at least 3 times and representative
155 results of one experiment are shown.

156 *2.5. Immunohistochemistry (IHC)*

157 Paraffin-embedded sections were deparaffinized and rehydrated in graded alcohols
158 using routine protocols. Briefly, sections (4 µm) were stained with anti-MRP4
159 antibody (Santa Cruz® biotechnologies, 1:100) with overnight incubation at 4°C.
160 Slides of adult colon were used as positive controls to test anti-MRP4 antibody.
161 Immunostaining was performed using the avidin-biotin-peroxidase complex
162 technique (Vectastain Elite ABC kit, Vector Laboratories, CA). The reactions were
163 developed with 3-3'diaminobenzidine (DAB) as described previously [24]. After
164 immunohistochemistry, the specimens were lightly counterstained with 10%
165 hematoxylin, dehydrated, and mounted. All negative controls were obtained by
166 excluding the primary antibody from the reaction. Slides were analyzed using light
167 microscopy by two independent investigators who were blinded to the patient data.
168 The immunohistochemical expression was evaluated and categorized in four
169 groups: negative (-), weak (+), moderate (++) and strong (+++) IHC expression.

170 2.6. *Cell lines and proliferation tests*

171 Two established human renal carcinoma cell lines Caki-1 and Caki-2 were used. The
172 former was derived from a human tumor skin metastasis, in opposition, Caki-2 was
173 established from a primary ccRCC. Both cell lines were grown in 25 cm² flasks at
174 37°C, in a humidified 5% CO₂ atmosphere, in DMEM medium supplemented with
175 10% fetal bovine serum, and 50 µg/mL gentamicin. HCT-116, cell line was use as
176 positive controls in RT-qPCR or immunocytochemistry (ICC) experiments. Cell
177 proliferation was measured by trypan blue staining and Neubauer chamber
178 counting or using the XTT[®] kit according to the manufacturer's instructions.

179 2.7. *Immunocytochemistry (ICC)*

180 Caki-1 or Caki-2 cells were grown on glass coverslips. The cells were washed with
181 1% BSA (Sigma-Aldrich) in PBS and permeabilized with Triton X100 (1%, PBS) for
182 5 min. Then, cells were incubated overnight at 4°C with primary anti-MRP4
183 antibodies (Santa Cruz[®] biotechnology; dilution 1:100). Incubations with a
184 secondary antibody, staining and scoring were done as previously described for IHC
185 assays.

186 2.8. *cAMP Radiobinding Protein Assay*

187 In all cases, cells were seeded in 24-well plates at a density of 1.10⁴ cells/well, and,
188 before starting each experiment, culture media was replaced with phenol red-free
189 media (Sigma-Aldrich) without FBS. Cells were then exposed to PBS (controls) or 25
190 µM Forskolin (FSK), and 1 mM 3-isobutyl-1-methylxanthine (IBMX) at different time
191 points as indicated in the corresponding figure legend. After treatment, at indicated
192 times, cell monolayer and supernatants were extracted with 95% v/v ethanol in
193 order to obtain intracellular cAMP (i-cAMP) and extracellular (e-cAMP) contents

194 respectively. Extracts were then evaporated, and residues were resuspended in
195 radiobinding protein (RBP) buffer (50 mM Tris-HCl, 4 mM EDTA, pH 7.4, 0.1% bovine
196 serum albumin). cAMP content was determined by a competitive RBP assay for PKA
197 using $^{[3H]}$ cAMP, as previously described [25]. Briefly, titrated PKA was incubated in
198 equilibrium conditions (2 hours, 4°C) with different samples or cAMP standards
199 (0.1–90 pmol) in the presence of 2 nM $^{[3H]}$ cAMP (20.7 Ci/mmol, NET1161250UC;
200 PerkinElmer) in RBP buffer. The bound fraction was separated by carbon–dextran
201 precipitation, followed by centrifugation (2000g, 15 minutes, 4°C), and Optiphase
202 HiSafe3 scintillation cocktail (PerkinElmer) was added to each supernatant for
203 counting in a Pharmacia Wallac 1410 counter. cAMP Sample concentrations were
204 determined by interpolating from the displacement curves obtained from cAMP
205 standards using Prism 8.0 (GraphPad Software). Duplicate samples of at least three
206 independent experiments were analyzed. For concentration–response assays, we
207 fit the pooled data from all experiments into a single equation.

208 2.9. Lipidomics approaches

209 Lipidomic determinations of the content of fatty acids (FA) in the triacylglycerides
210 (TAG) and cholesterol esters (CE) fractions were determined using gas
211 chromatography coupled to mass spectrometry (GC-MS) according to the
212 procedures previously described [26]. Analysis of eicosanoids by LC/MS was carried
213 out exactly as described elsewhere [27], using an Agilent 1260 Infinity high-
214 performance liquid chromatograph equipped with an Agilent G1311C quaternary
215 pump and an Agilent G1329B Autosampler, coupled to an API2000 triple
216 quadrupole mass spectrometer (Applied Biosystems, Carlsbad, CA, USA).
217 Quantification was carried integrating the chromatographic peaks of each species

218 and by comparing with an external calibration out by integrating the
219 chromatographic peaks of each species and by comparing with an external
220 calibration curve made with analytical standards [28].

221 *2.10. Cell cycle assessment*

222 Caki-2 cells were seeded in a 6-well plate at 2.5×10^5 cells/well. After treatments,
223 cells were washed with PBS and harvested using Tripsin-EDTA (GIBCO) and then
224 fixed with cold Ethanol 70% and a final concentration was adjusted to 10^6 cells/mL.
225 The cells were treated with RNase A (Sigma, Darmstadt, Germany) for 15 minutes
226 at 37°C and stained using propidium iodide (PI) 1 mg/mL (Sigma, Darmstadt,
227 Germany) for 15 minutes. The DNA content of the cells were analyzed using
228 FACSCalibur (BD Biosciences, San Jose, CA, USA) and the data was analyzed with
229 FlowJo (BD Biosciences, San Jose, CA, USA).

230 *2.11. Confocal microscopy*

231 The cells were plated on coverslips and then fixed with 4% paraformaldehyde in PBS
232 containing 3% sucrose for 20 min. Afterward, paraformaldehyde was removed by
233 washing the cells thrice with PBS, and BODIPY493/503 (2 µg/ml) and DAPI (1 µg/ml)
234 staining were carried out. Coverslips were mounted on microscopy slides with 25 µl
235 of a polyvinyl alcohol solution until analysis by fluorescence microscopy. Lipid drops
236 were analyzed using oleic acid (30 µM) as a positive control. In contrast, untreated
237 cells were used as negative controls. Fluorescence was monitored by microscopy
238 using a confocal BioRad laser scanning system Radiance 2100. Images were analyzed
239 with the ImageJ software (NIH; Ver 1.52a).

240

241

242 2.12. Statistics

1
2 243 Statistics were performed using GraphPad Prism 8.0 via an unpaired *t* test or one-
3
4 244 way analysis of variance (ANOVA) followed by Bonferroni's or Tukey's comparison
5
6
7 245 test. Differences were considered statistically significant at $p < 0.05$.
8

9 246

10
11
12 247 **3. Results**

13
14 248 3.1. *MRP4 is overexpressed in ccRCC*

15
16
17 249 MRP4 is an apical organic anion transporter and the known efflux pump for cAMP
18
19
20 250 in human kidney proximal tubules [29]. While MRP4 extrudes drugs to the proximal
21
22 251 tubular lumen and metabolites from the cellular cytoplasm, OATP4C1 has a reverse
23
24
25 252 flow of substance transport [14,30]. In order to establish the implication that the
26
27 253 rate of both transporters would have as cellular modulators of cAMP, we first
28
29
30 254 performed an *in-silico* analysis to determine the level of expression of MRP4 and
31
32 255 OATP4C1 mRNAs in ccRCC and normal patients, using specific probes as described
33
34
35 256 in materials and methods.

36
37
38 257 MRP4 showed a clear overexpression in tumors (n=69), in comparison with normal
39
40 258 patients (n=32; difference of median 169.3; $P < 0.0001$). In opposition, OATP4C1
41
42
43 259 showed lower expression levels than normal samples (**Figure 1A**). This opposite
44
45 260 expression of both proteins could explain the peculiar phenotype exhibited by these
46
47
48 261 tumors. In parallel, the overexpression of MRP4 could mean a hyper-functionality,
49
50
51 262 susceptible of being treated therapeutically. Thus, we focused on MRP4. We next
52
53 263 evaluated the expression and localization of this protein in human tumor samples
54
55
56 264 of ccRCC. First, we determined the expression level of MRP4 mRNA transcripts in
57
58
59 265 renal control samples and tumors by RT-qPCR. ccRCC tumors are solid and compact

266 tissue masses with distinguishable macroscopic features between the center and
267 the periphery of the tumor. While the center shows a high lipid content, the
268 periphery of the tumor exhibits abundant fibrous tissue with less friable
269 consistency. In order to determinate the MRP4 expression profile, we analyzed the
270 protein expression in two different areas of the tumor mass: *Core* (center) and
271 *Periphery* (other zones in the border) (n=18). **Figure 1B** shows that the expression
272 level of this messenger in the aforementioned tumoral sections, is at least 20-fold
273 higher than in normal tissues, considering the core (media= 47.46) and periphery
274 (media= 21.34). Similarly, when we analyzed the expression levels of the protein in
275 tumors, in all analyzed cases we found at least 5-10-fold increase, when compared
276 to the control samples (**Figure 1B**).

277 Immunohistochemical staining was tested to confirm the enhanced MRP4
278 expression and to determine its sub-cellular localization (**Figure 1C-J**). First, we
279 investigated the MRP4 expression in non-neoplastic tissues (Normal; n=10). This
280 protein showed a homogeneous and intense membranous pattern in all samples.
281 MRP4 was circumscribed only to the renal proximal tubular cells, since a complete
282 absence was observed in the glomerular components (**Figure 1C and F**). On the
283 other hand, tumoral MRP4, displayed a very strong and rather heterogeneous
284 expression with zone-dependent differences: high levels (score 2+ or 3+) of
285 membranous MRP4 expression in the core (80 %) and in contrast, mild and
286 moderate protein expressions (score +1 or 2+) in peripheral tissues (100%; **Figure**
287 **1J**). Additionally, **Figure 1C-E and F-H** illustrate two patients with different
288 expression levels of MRP4. The first one shows a more balanced expression of the

289 protein between sectors, while the second denotes clear differences between the
290 core and the periphery (Panels **D-E** and **G-H** respectively).

291 Opposite to the observations in peripheral tissues, tumor core shows a high
292 heterogeneous expression of this protein with intense foci (arrows)(**Figure 1J**).

293 → **Figure 1**

294 3.2. *MRP4 expression in renal cell lines: Caki-1 and Caki-2*

295 Given the differential expression of MRP4 in tumors and normal tissue, we set out
296 to design a model that allows us to validate this protein as a therapeutic target or a
297 prognosis marker. We measured the expression level of this protein in the two cell
298 lines representing ccRCC with dissimilar degrees of differentiation. Caki-1 is a cell
299 line derived from a metastatic skin clear cell renal carcinoma tumor (well-
300 differentiated) and Caki-2 is another human clear cell renal carcinoma line that also
301 displays epithelial morphology and grows in adherent culture (less-
302 differentiated)[31,32]. Following the same rationale used in IHQ (**Figure 1I**), we used
303 HCT-116, a colonic tumoral cell line, as positive control to measure the basal
304 expression of MRP4. **Figure 2A** shows that Caki-2 is the cell line that displays the
305 maximum expression of MRP4 mRNA (~3-fold higher than Caki-1 cells). Monolayers
306 from these cell lines were scraped and proteins were extracted for western blot
307 analysis. **Figure 2B** shows that both cell lines exhibit MRP4 but clearly, Caki-2 cells
308 express 1.5-fold increased. This difference was analyzed and quantified as shown in
309 materials and methods using ImageJ software (**Figure 2C**).

310 Similarly to previous assays, MRP4 expression was also confirmed by **ICC**. No
311 quantitative differences in protein expression were observed nor specific
312 localizations between Caki cell lines. Cytoplasmic aggregates of proteins were found
313

314 in Caki cells (light blue and red arrows), in opposition to the remarkable
315 membranous pattern observed for HCT-116 cells (Black arrows; **Figure 2D**).

316 → **Figure 2**

317

318 **3.3. cAMP efflux is mediated by MRP4 in Caki-1 and Caki-2 cells and it is engaged in cell**
319 ***proliferation***

320 MRP4 has been described as the main transporter involved in cAMP extrusion in
321 other cancer cell lines [17,18]. Thus, we next evaluated cAMP dynamics in Caki-1
322 and Caki-2 cells by kinetic experiments. To study the efflux and intracellular
323 accumulation of cAMP, Caki cell lines were treated with IBMX (1 mM), a
324 phosphodiesterase (PDE) inhibitor and FSK (25 μ M), an adenylyl cyclase direct
325 activator. Then the supernatant or scraped cells were collected for the radiometric
326 measurement of extracellular cAMP (e-cAMP) and intracellular cAMP (i-cAMP)
327 respectively as it was previously described in M&M. Thus, in order to show
328 differences in the extrusion capacity of this nucleotide for both lines, we calculated
329 the area under the curve (AUC) values for both e-cAMP and i-cAMP levels and
330 plotted their ratio (**Figure 3A**). Caki-2 cells presented the highest AUC e-cAMP/AUC
331 i-cAMP, in contrast with Caki-1 (difference between means 0.073; $P= 0.007$).
332 Strikingly, the ratio between both extrusion capacities is approximately 1.36 ± 0.07 ,
333 which is in agreement with the protein difference found by western blotting or even
334 more by RT-qPCR, for both cell lines.

335 To further characterize cAMP efflux, Caki cells were incubated in the
336 aforementioned experimental conditions (IBMX + FSK), and also two different MRP4
337 inhibitors: MK-571 (25 μ M; 5 min) or Probenecid (0.5 mM; 5 min) were added. The
338 synergistic effect of increased cAMP synthesis, inhibition of its degradation and

339 simultaneous inhibition of its extrusion, produced a significant rise in the
1 340 accumulation of i-cAMP compared to controls in Caki-2. As seen in **Figure 3B**, the
2
3 341 pharmacological inhibition of MRP4 leads to significant decreases in the e-cAMP
4
5 342 levels in both cell lines, denoting an effective inhibition of the extrusion of this
6
7 343 metabolite. In summary, these results indicate that that MRP4 is the carrier
8
9 344 responsible for modulating cAMP levels in both, intra and extracellular space, in
10
11 345 Caki-2 cell line. In light of the above observations, we next investigated the role of
12
13 346 MRP4 in ccRCC proliferation. If the extrusion of cAMP was directly related to the
14
15 347 amount of MRP4 expressed, the Caki-2 cells would proliferate with greater speed
16
17 348 [15,18]. Effectively, in all the developed experiments we have observed that Caki-2
18
19 349 innately proliferates faster (**Figure 3C**). Additionally, in order to demonstrate that e-
20
21 350 cAMP is engaged in proliferation, cells were depleted from FBS-supplemented
22
23 351 medium and different concentrations of this cyclic nucleotide were added to the
24
25 352 culture medium and then cell proliferation was evaluated (**Figure 3D**). Low cAMP
26
27 353 concentrations (such as 10 μ M) induced up to 100% increase in proliferation in Caki-
28
29 354 2 cells. Simultaneously, this effect seems to have a saturation limit, since no dose-
30
31 355 dependent effect was observed. Strikingly, Caki-2 cells, which extrude more cAMP,
32
33 356 better show this responding effect to e-cAMP. Similar results were obtained when
34
35 357 cell proliferation was evaluated using both Neubauer chamber or XTT cell
36
37 358 proliferation Kit[®]. Additionally, Caki-2 cells were treated with cAMP (10 μ M) and cell
38
39 359 cycle stages were analyzed using flow cytometry. Treated cells showed a significant
40
41 360 increase in Phase S (35.43%) compared to control cells (**Figure 3E**).

56 361 → **Figure 3**

58 362

363 3.4. *The pharmacological inhibition of MRP4 activity induce phenotypical changes,*
364 *inhibits Caki cell proliferation and finally triggers apoptosis cell death*

365 Previous reports showed that the e-cAMP/i-cAMP balance is crucial for cell
366 proliferation[18]. The increase in i-cAMP induces proliferation inhibition associated
367 with cell differentiation in AML [17], and decrease in i-cAMP is associated with cell
368 growth inhibition and cell cycle arrest in PDAC models [18]. Considering that it is
369 pharmacologically possible to modulate the e-cAMP/ i-cAMP balance (**Figure 3**), we
370 next investigated its biochemical cellular effects. Since the Caki-2 line has a greater
371 degree of undifferentiation (increased proliferative capacity and malignancy),
372 greater expression of MRP4 and, consequently, greater cAMP extrusion capacity or
373 accumulation of i-cAMP (if MRP4 is inhibited), we focused on this renal cell line.

374 When Caki-2 cells were exposed to MK-571 (25 μ M; selective pharmacological
375 inhibitor of MRP4) and simultaneously stimulated the production of i-cAMP with
376 FSK (25 μ M) for 18-24 h, they showed very clear changes in cell morphology
377 (cytoplasmic stretching and cell thinning) compatible with cell stress
378 (**Supplementary Figure 1**). We and others [33] have shown that a remarkable
379 measure of cellular stress assessment is the observation of lipid droplets (LD). Using
380 different approaches, such as flow cytometry analysis and confocal microscopy, we
381 determined that the number of LD increases under the experimental conditions
382 mentioned above. **Figure 4A-C** shows an increase in the media fluorescence
383 intensity (MFI) of treated cells (MK-571 + FSK, both 25 μ M) compared to control
384 cells (difference between means: $81,33 \pm 5,81$; $P= 0.0002$), after staining them with
385 Bodipy[®], a specific LD dye. Simultaneously, Caki-2 cells were observed with confocal
386 microscopy using oleic acid (OA; 30 μ M) as positive control for the LD biogenesis

387 [34,35]. While the OA-induced LDs, show an apical order denoting a cellular
388 polarization, the microscopic image of the cells treated with the MRP4 inhibitor and
389 FSK showed rather a cytoplasmic profile distribution of the fluorescence,
390 compatible with a greater number of smaller LD (**Figure 4D-F**).

391 → **Supplementary Figure 1**

392 In order to determine if the biochemical composition of these LDs had quantitative
393 differences, we analyzed the lipidomic profile of fatty acids (FA) in phospholipids
394 (PLs), triacylglycerides (TAG) and cholesterol esters (CE) fractions using GC-MS.
395 **Figure 4G** panels show greater accumulation of saturated fatty acids, mainly 16:0
396 and 18:0 (palmitic acid and stearic acid respectively) in both TAG and CE fractions,
397 on cells simultaneously treated with FSK and MK-571. In contrast, the PLs fraction
398 showed no major changes in FA composition between treated cells and controls
399 (**Supplementary Figure 2**).

400 → **Supplementary Figure 2**

401 Longer treatment times, beyond 24 h, and even only exposed to MRP4 inhibitor
402 (MK-571 or Probenecid) drastically affected the cells and progressively, an impaired
403 proliferative capacity was observed (**Figure 4H**). The compromised cell proliferation
404 observed at 48 h is compatible with the increase in the Sub G₀ stage of cells under
405 the same experimental conditions (19.1%) analyzed by flow cytometry (**Figure 4I**).
406 Evidently, the MRP4 pharmacological inhibition, resulted in apoptosis, as revealed
407 by morphological changes (membrane bubbles) observed by optical and electron
408 microscopy (data not shown) and by activation of caspases (Caspase-3; apoptosis
409 effector pathway) measured by ICC (**Figure 4J**).

410 Different chemotherapeutic drugs and endogenous physiological mediators, such
411 as eicosanoids, have been previously reported as important substrates of MRP4

1
2
3
4
5
6
7
8
9
10
11
12
13
14
15
16
17
18
19
20
21
22
23
24
25
26
27
28
29
30
31
32
33
34
35
36
37
38
39
40
41
42
43
44
45
46
47
48
49
50
51
52
53
54
55
56
57
58
59
60
61
62
63
64
65

412 [12]. In order to determine if any others MRP4 substrate metabolites, in addition to
413 cAMP, could accumulate in the cytoplasmic compartment and subsequently
414 interfere with cell proliferation, we measured the profile of eicosanoids in Caki-2
415 cells under the experimental conditions outlined above. Using solid phase
416 extraction and HPLC coupled to tandem mass spectrometry (TQP), we determined
417 a set of 20 eicosanoids in the intracellular fractions and in the cell culture
418 supernatant. Then, we evaluated their production in a wide range of temporal
419 exposure (1-24 h). After an exhaustive analysis, we did not found differences in the
420 profile of eicosanoids in the intracellular space. By contrast, the extracellular space
421 does show the accumulation of some eicosanoids such as 12-HETE, tetranor-12-
422 HETE and 14-HDoHE. This is more obvious at 18 h of exposure, at which time we
423 have already shown that cellular stress begins and subsequently the consequent cell
424 death by apoptosis (24 h) (**Supplementary Figure 3**). These results are compatible
425 with the hypothesis that cAMP is the metabolite hitherto mainly involved in the
426 biological effects previously described.

427 Taking together, all these data suggest that, an inhibition of MRP4 function leads to
428 an imbalance of MRP4 substrates and this provokes an inhibition of cell proliferation
429 and subsequently induction of apoptosis. Simultaneously this pharmacological
430 inhibition caused phenotypic changes associated to the cellular lipid profile.

431 → **Figure 4**

432 → **Supplementary Figure 3**

433 3.5. *MRP4 is overexpressed under hypoxic conditions*

434 We have already shown that MRP4 has a differential expression pattern in tumors
435 versus normal tissues, and we also observed that there is a heterogeneous
436 expression of MRP4 in intratumoral sectors: MRP4 has greater expression in the

437 core than in the periphery. In addition, unpublished data from our laboratory
1 438 suggests that the core cells of this tumor show greater mitotic capacity than those
2
3
4 439 from the periphery (measured by Ki-67 expression). In line with this idea, our Caki
5
6 440 cell model showed that there is a direct association between the level of MRP4
7
8 441 expression and the proliferation capacity of these cell lines. On the other hand,
9
10 442 numerous reports indicate that cells in the tumor core are often in hypoxia due to
11
12 443 their impaired ability to access blood capillaries [36,37]. Considering all of the
13
14 444 above, we set out to investigate whether there is a direct association between both
15
16 445 phenomena: Hypoxia and MRP4 expression. In order to develop this, we previously
17
18 446 designed a chemical hypoxia assay by treatment of Caki-2 cells with CoCl₂ [38,39].
19
20 447 First, we determined the range of non-cytotoxic concentrations of this salt for Caki-
21
22 448 2 cells (**Figure 5A**). Subsequently, we evaluated whether these experimental
23
24 449 conditions represent a hypoxic micro-environment, confirming the increased
25
26 450 expression of HIF-2 α by both qPCR (**Figure 5B**) and ICC (**Figure 5C-D**). We observed
27
28 451 that the control cells showed a weak and homogeneous cytoplasmic staining
29
30 452 pattern, in contrast to treated cells (eg. 300 μ M) that show HIF-2 α nuclear
31
32 453 translocation and exhibit a marked perinuclear or nuclear expression (**Figure 5D**,
33
34 454 arrows).

455 In this context, in the experimental conditions mentioned above, we found a dose-
46
47 456 dependent increase in MRP4 mRNA. Particularly with 300 μ M CoCl₂, we detected a
48
49 457 10-fold increase (**Figure 5E**). Higher concentrations involve cell cytotoxicity and this
50
51 458 probably explain the lower MRP4 mRNA expression at 400 μ M.

52
53
54
55
56 459 → **Figure 5**

57
58
59 460

1
2
3
4
5
6
7
8
9
10
11
12
13
14
15
16
17
18
19
20
21
22
23
24
25
26
27
28
29
30
31
32
33
34
35
36
37
38
39
40
41
42
43
44
45
46
47
48
49
50
51
52
53
54
55
56
57
58
59
60
61
62
63
64
65

461 4. Discussion

1
2 462 Despite the therapeutic advances achieved using combinations of TK receptor inhibitors
3
4 463 and / or immunotherapy, kidney cancer still causes more than 100,000 deaths a year
5
6 464 worldwide. Due to the aforementioned mortality, it is urgent to develop reliable, safe
7
8
9 465 and effective therapeutic strategies based on the mechanisms that govern this
10
11 466 pathology [4,40].

12
13
14 467 It has long been known that the mechanisms of resistance acquired by tumors are based
15
16
17 468 on the existence of efflux proteins dependent on the ATP hydrolysis (ABCs)[9,41].
18
19 469 Among them, MRP4 has been described as responsible for chemoresistance or essential
20
21
22 470 for cell proliferation in many tumors, such as Pancreas [42], Neuroblastoma [8], Acute
23
24
25 471 myeloid leukemia [17], Lung [7], Ovarium [43], Esophagus [44], Colon [45,46] as well as
26
27 472 a prognostic marker due to its overexpression compared to normal tissues [43,47].

28
29
30 473 While other MRPs have been reported overexpressed in different types of tumors, in
31
32 474 this work to the best of our knowledge, we report for the first time, that MRP4 is
33
34
35 475 overexpressed in ccRCC.

36
37
38 476 Thus, using search algorithms in virtual platforms, we developed an *in-silico* analysis of
39
40 477 the mRNA expression of two transporters with opposite direction of pumping: MRP4
41
42 478 and OATP4C1 [48]. As shown in the obtained results, the combination of the
43
44
45 479 overexpression of MRP4 and the downregulation of OATP4C1 shows the ideal scenario
46
47
48 480 to propose MRP4 as a possible target of pharmacological action. In this sense, all ccRCC
49
50
51 481 tumors examined in this study were found to express MRP4, and its overexpression was
52
53 482 significantly high. This is very distinguishable, since normal renal tissues exhibit low
54
55
56 483 MRP4 levels. A proteomic study that evaluated all functional transporters in the healthy
57
58
59 484 renal cortex, showed that MRP4 is expressed at a very low level (less than 1 pg/mg.

60
61
62
63
64
65

485 Protein), which is in line with the western blotting made in this work [49]. Thus, the
1 486 MRP4 overexpression observed is comparable to those detected in pancreas [18,42],
2
3 487 colon [46], osteosarcoma [50] tumors and it seems to be far above compared to
4
5 488 leukemia [51] or lymphoma [52].
6
7 489 ccRCC tumors characteristically show a bright yellow color in the center as a result of its
8
9 490 abundant lipid content, and a variegated appearance in the border with hemorrhage,
10
11 491 necrosis and/or fibrosis with a well-circumscribed capsule or pseudo-capsule that
12
13 492 separates the tumor from adjacent tissues [53]. Since that, we arbitrarily separated the
14
15 493 tumor into two zones: *Core* and *Periphery*, and we focused on the analysis of the
16
17 494 expression of MRP4 in both zones. We observed a marked heterogeneity of expression
18
19 495 of this transporter along tumor tissues, something already described for MRP4 in tumors
20
21 496 like prostate [47].
22
23 497 Given the possible therapeutic implications that have been described for MRP4 in other
24
25 498 cancer cells, and in order to develop some functional test, we studied its expression in
26
27 499 cell lines to validate a model for this transporter. As mentioned before, we first used
28
29 500 two cell lines with different degrees of differentiation, Caki-1 obtained from a skin
30
31 501 metastasis of renal carcinoma (well-differentiated)[31], and Caki-2 cell line model of
32
33 502 clear cell renal carcinoma (less-differentiated)[32,54]. Thus, in line with what was
34
35 503 observed by Carozzo and collaborators, who analyzed the correlation between the
36
37 504 degree of differentiation and the expression of MRP4 in three pancreatic cancer cell
38
39 505 lines [18], we observed that MRP4 levels in Caki-2 are slightly higher than those of Caki-
40
41 506 1 in both mRNA and protein. Similarly the same trend was observed in leukemias [17,51]
42
43 507 and lymphomas [52], where the malignancy and the degree of dedifferentiation are
44
45 508 remarkably linked.
46
47
48
49
50
51
52
53
54
55
56
57
58
59
60
61
62
63
64
65

509 Since both Caki lines express MRP4, we next evaluated their functional faculty to extrude
1 510 cAMP in *in vitro* cultures. As expected, Caki-2 showed a higher extrusion capacity (~30%)
2
3 511 of cAMP confirming that this cell line actually shows a greater amount of MRP4.
4
5
6 512 Additionally, we confirmed the responsibility for extrusion of this cyclic nucleotide by
7
8
9 513 MRP4, using selective pharmacological inhibitors of this carrier. Thus, we abolished the
10
11
12 514 role that MPR4 possesses to modulate cAMP levels both in the intra and extracellular
13
14
15 515 compartments. Based on these findings, as shown in results, Caki-2 proliferates faster,
16
17 516 as demonstrated using XTT reagent. These data confirmed that, also in renal carcinomas,
18
19
20 517 a higher expression of MRP4 is associated with higher cell duplication rate and in
21
22 518 consequence, greater malignancy.
23
24
25 519 Different studies show that MRP4, MRP5, and MRP8 induce the extrusion of cyclic
26
27 520 nucleotides in various cell types; however, MRP4 has emerged as the main transporter
28
29
30 521 for cAMP [12]. In this sense, Copsel and collaborators, further characterized cAMP efflux
31
32 522 by MRP4, in human myeloid leukemia cells and the effect of its pharmacological
33
34
35 523 blockade on cell proliferation and differentiation to a non-neoplastic phenotype [17].
36
37
38 524 This inspired us to use the same model of pharmacological inhibition to modulate the
39
40 525 cAMP pathway in renal carcinoma. In fact, both inhibitors, probenecid and MK-571,
41
42
43 526 were effective to increase the concentration of i-cAMP or depleting the extracellular
44
45
46 527 medium of it, and therefore, decline cell proliferation in Caki-2 cells (see below). This
47
48 528 pharmacological model was verified for other types of cancer, and also using shRNA
49
50
51 529 technology, this transporter was silenced or overexpressed and thus cAMP levels could
52
53 530 be modulated, leading to equivalent results [18]. These data allowed us to assume, that
54
55
56 531 similar to what was observed in leukemia and pancreas carcinoma, cAMP has a dual role
57
58
59 532 in ccRCC depending on its compartmentalization (extra o intracellular). Thus, our data
60
61
62
63
64
65

533 and those obtained by others, would allow us to infer that e-cAMP induce cell
1 534 proliferation and on the other hand, uncontrolled increments of i-cAMP would induce
2
3
4 535 cell stress and apoptosis.
5

6 536 Ultrastructural features reported for Caki-2 cells include microvilli and microfilaments
7
8
9 537 with few mitochondria, and abundant LD [55]. As mentioned before, a remarkable
10
11 538 characteristic of the phenotype of ccRCC is their high lipid content [53] with specific
12
13 539 lipidomic signatures [21], so the cell lines that represent it, also exhibit these lipid-filled
14
15 540 organelles. LDs are formed under very different conditions but undoubtedly cellular
16
17 541 stress or an imbalance in lipid metabolism are basic pathognomonic signs that trigger
18
19 542 the biogenesis of these organelles. In these cases, it is hypothesized that fatty acids in
20
21 543 LDs may serve as protectors against the stressors [33,56]. The combination of drugs used
22
23 544 in our model (FSK and/or inhibitors) to rise i-cAMP, induced remarkable cellular
24
25 545 morphological changes, already visible only with optical microscopy in the first hours of
26
27 546 exposure. A further analysis of the cells under these conditions, using flow cytometry
28
29 547 and confocal microscopy, confirmed the LDs biogenesis. Additionally, we also performed
30
31 548 a lipidomic analysis and determined the FA content of LD. Cells treated with FSK alone
32
33 549 underwent a marked thinning and showed much lower number of LD compared to
34
35 550 control cells. Although there was an apparent decrease of 16:0, 18:0 and 18:1, no
36
37 551 significant statistical variations were found. Something similar occurs with the decrease
38
39 552 in size in LD stimulated with FSK in 3T3-L1 adipocytes [57].
40
41
42
43
44
45
46
47
48
49
50

51 553 When the cells were treated with the combination of FSK + MK-571, similar morphologic
52
53 554 changes (stretching and cell thinning) were observed to those only treated with FSK.
54
55 555 However, significant increases were detected in TAG and CE fractions in these cells,
56
57 556 demonstrating, that it is the inhibition of the function of MRP4 that generates the
58
59
60
61
62
63
64
65

557 change of cellular lipid composition. First, we thought that in consonance to what was
1 558 found for other cell lines (*e.g.* myeloid leukemia), these experimental conditions tended
2
3
4 559 to induce a cellular differentiation towards a non-neoplastic phenotype similar to
5
6
7 560 adipocytes. However, we observed that prolonged exposure times to FSK + MK-571,
8
9
10 561 induces apoptosis [58,59].

11 562 Although the idea of cell transdifferentiation to an adipocyte-like phenotype is an
12
13
14 563 attractive research option, there are controversies. Several studies have shown that
15
16
17 564 tumor cells reactivate *de novo* lipid synthesis [60] and particularly, Saito and
18
19
20 565 collaborators using an untargeted lipidomic approach clearly showed that CE and TAG
21
22
23 566 are accumulated in ccRCC tumor tissues [21]. However, our data shows that when this
24
25
26 567 increase in lipid biosynthesis is achieved in combination with the blockade of MRP4, the
27
28
29 568 cells stop their proliferation and trigger cell apoptosis. So, it remains to be determined
30
31
32 569 whether the increase in lipid synthesis in these tumor cells is positive or not.

33 570 Another key point that intertwines and governs many important essential metabolic
34
35
36 571 processes in tumor cells is hypoxia. We previously described the relationship among
37
38
39 572 proliferation, survival, and apoptosis with the expression of key molecules related to
40
41
42 573 tumoral hypoxia in ccRCC tumors (hypoxia-inducible factor (HIF)-1 α , erythropoietin
43
44
45 574 (EPO), vascular endothelial growth factor (VEGF), and their receptors (EPO-R, VEGFR-2)
46
47
48 575 [24]. In addition, in this work we also showed that MRP4 is upregulated in these tumors.
49
50
51 576 Thus, we investigated whether there is a direct relationship between both phenomena,
52
53
54 577 in order to know if MRP4 function is also engaged with the phenotype of this tumor. We
55
56
57 578 demonstrated that, in the chemical hypoxia model set up, MRP4 exhibited a significant
58
59
60 579 increase in expression. Although this is a novel data for ccRCC, it is perfectly consistent
61
62
63 580 with the previous data obtained since that: **a)** we observed a differential expression of
64
65

581 MRP4 in core and peripheral in ccRCC tumors; **b)** there is an increased expression of
582 hypoxia markers in the core; **c)** tumor cells exhibit an increased proliferative capacity
583 under hypoxia conditions; and **d)** we observed a higher expression of MRP4 in Caki-2
584 cells, which are the ones cells with the greatest proliferative capacity.

585 Although these results are preliminary and additional experiments are needed to
586 determine the mechanism of activation of the synthesis of MRP4, these findings would
587 indicate that the target points that regulate hypoxia could modulate the expression of
588 MRP4 and in consequence cAMP levels.

589 All in all, data presented herein show direct evidence that MRP4 is a differential marker
590 in solid ccRCC tumors, which is involved in the cAMP signaling pathway and therefore,
591 could be a new pharmacological target to be employed in therapeutic strategies for the
592 treatment of ccRCC so far not addressed.

593

594 **5. Acknowledgements**

595 The authors thank Montse Duque for the excellent technical assistance.

596

597 **6. Author contributions**

598 **Juan Pablo Melana Colavita:** Conceptualization, Methodology, Writing. **Maximiliano de**
599 **Sousa:** Software. **Juan Santiago Todaro, Leandro Ferrini, María May, Carlos Guijas,**
600 **Natalia Gomez, Agustin Yaneff, Nicolas Di Siervi:** Methodology, Supervision, Data
601 Curation. **María Victoria Aguirre, Carlos Davio** and **Juan Pablo Rodríguez:**
602 Conceptualization, Writing- Reviewing, Editing and Project administration.

603

604

1
2
3
4
5
6
7
8
9
10
11
12
13
14
15
16
17
18
19
20
21
22
23
24
25
26
27
28
29
30
31
32
33
34
35
36
37
38
39
40
41
42
43
44
45
46
47
48
49
50
51
52
53
54
55
56
57
58
59
60
61
62
63
64
65

605 **7. Funding**

606 This research was funded by Universidad Nacional del Nordeste, SGCyT-UNNE PI18-I009;
607 UBACYT-20020170100674BA-2018 and MINCYT-FONCYT- PICT-2015-2996.

608

609 **8. Conflict of Interest Statement**

610 The authors declare no conflict of interest. The funders had no role in the design of the
611 study; in the collection, analyses, or interpretation of data; in the writing of the
612 manuscript, or in the decision to publish the results

613

614 **9. References**

- 615 [1] K. Wang, Y. Sun, W. Tao, X. Fei, C. Chang, Androgen receptor (AR) promotes clear
616 cell renal cell carcinoma (ccRCC) migration and invasion via altering the
617 circHIAT1/miR-195-5p/29a-3p/29c-3p/CDC42 signals, *Cancer Lett.* 394 (2017) 1–12.
618 doi:10.1016/j.canlet.2016.12.036.
- 619 [2] B. Greef, T. Eisen, Medical treatment of renal cancer: New horizons, *Br. J. Cancer.*
620 115 (2016) 505–516. doi:10.1038/bjc.2016.230.
- 621 [3] Z.F. Bielecka, A.M. Czarnecka, W. Solarek, A. Kornakiewicz, C. Szczylik, Mechanisms
622 of Acquired Resistance to Tyrosine Kinase Inhibitors in Clear - Cell Renal Cell
623 Carcinoma (ccRCC), *Curr Signal Transduct Ther.* 8 (2014) 218–228.
624 doi:10.2174/1574362409666140206223014.
- 625 [4] R.J. Motzer, E. Jonasch, M.D. Michaelson, L. Nandagopal, J.L. Gore, S. George, A.
626 Alva, N. Haas, M.R. Harrison, E.R. Plimack, J. Sosman, N. Agarwal, S. Bhayani, T.K.
627 Choueiri, B.A. Costello, I.H. Derweesh, T.H. Gallagher, S.L. Hancock, C.
628 Kyriakopoulos, C. LaGrange, E.T. Lam, C. Lau, B. Lewis, B. Manley, B. McCreery, A.

- 629 McDonald, A. Mortazavi, P.M. Pierorazio, L. Ponsky, B.G. Redman, B. Somer, G.
1
2 630 Wile, M.A. Dwyer, L.J. Hammond, G. Zuccarino-Catania, NCCN Guidelines Insights:
3
4 631 Kidney Cancer, Version 2.2020, J. Natl. Compr. Cancer Netw. 17 (2019) 1278–1285.
5
6 632 doi:10.6004/jnccn.2019.0054.
7
8
9 633 [5] A. Ivanyuk, F. Livio, J. Biollaz, T. Buclin, Renal Drug Transporters and Drug
10
11 634 Interactions, Clin. Pharmacokinet. 56 (2017) 825–892. doi:10.1007/s40262-017-
12
13 635 0506-8.
14
15
16 636 [6] J. Wen, J. Luo, W. Huang, J. Tang, H. Zhou, W. Zhang, The Pharmacological and
17
18 637 Physiological Role of Multidrug-Resistant Protein 4, J. Pharmacol. Exp. Ther. 354
19
20 638 (2015) 358–375. doi:10.1124/jpet.115.225656.
21
22
23 639 [7] X. Zhao, Y. Guo, W. Yue, L. Zhang, M. Gu, Y. Wang, ABCC4 is required for cell
24
25 640 proliferation and tumorigenesis in non-small cell lung cancer, Onco. Targets. Ther.
26
27 641 7 (2014) 343–351. doi:10.2147/OTT.S56029.
28
29
30 642 [8] T. Huynh, M.D. Norris, M. Haber, M.J. Henderson, ABCC4/MRP4: a MYCN-regulated
31
32 643 transporter and potential therapeutic target in neuroblastoma, Front. Oncol. 2
33
34 644 (2012) 1–7. doi:10.3389/fonc.2012.00178.
35
36
37 645 [9] Y.-K. Zhang, Y.-J. Wang, P. Gupta, Z.-S. Chen, Multidrug Resistance Proteins (MRPs)
38
39 646 and Cancer Therapy, AAPS J. 17 (2015) 802–812. doi:10.1208/s12248-015-9757-1.
40
41
42 647 [10] T. Belleville-Rolland, Y. Sassi, B. Decouture, E. Dreano, J.S. Hulot, P. Gaussem, C.
43
44 648 Bachelot-Loza, MRP4 (ABCC4) as a potential pharmacologic target for
45
46 649 cardiovascular disease, Pharmacol. Res. 107 (2016) 381–389.
47
48 650 doi:10.1016/j.phrs.2016.04.002.
49
50
51 651 [11] Y.H. Liu, Y.M. Di, Z.W. Zhou, S.L. Mo, S.F. Zhou, Multidrug resistance-associated
52
53 652 proteins and implications in drug development, Clin. Exp. Pharmacol. Physiol. 37
54
55
56
57
58
59
60
61
62
63
64
65

- 653 (2010) 115–120. doi:10.1111/j.1440-1681.2009.05252.x.
- 1
2 654 [12] F.G.M. Russel, J.B. Koenderink, R. Masereeuw, Multidrug resistance protein 4
3
4 655 (MRP4/ABCC4): a versatile efflux transporter for drugs and signalling molecules,
5
6 656 Trends Pharmacol. Sci. 29 (2008) 200–207. doi:10.1016/j.tips.2008.01.006.
7
8
9 657 [13] J. Wen, J. Luo, W. Huang, J. Tang, H. Zhou, W. Zhang, The Pharmacological and
10
11 658 Physiological Role of Multidrug-Resistant Protein 4, J. Pharmacol. Exp. Ther. 354
12
13 659 (2015) 358–375. doi:10.1124/jpet.115.225656.
14
15
16
17 660 [14] T. Mikkaichi, T. Suzuki, T. Onogawa, M. Tanemoto, H. Mizutamari, M. Okada, T.
18
19 661 Chaki, S. Masuda, T. Tokui, N. Eto, M. Abe, F. Satoh, M. Unno, T. Hishinuma, K. -i.
20
21 662 Inui, S. Ito, J. Goto, T. Abe, Isolation and characterization of a digoxin transporter
22
23 663 and its rat homologue expressed in the kidney, Proc. Natl. Acad. Sci. 101 (2004)
24
25 664 3569–3574. doi:10.1073/pnas.0304987101.
26
27
28
29 665 [15] A. Yaneff, A. Sahores, N. Gómez, A. Carozzo, C. Shayo, C. Davio, MRP4/ABCC4 As a
30
31 666 New Therapeutic Target: Meta-Analysis to Determine cAMP Binding Sites as a Tool
32
33 667 for Drug Design, Curr. Med. Chem. 26 (2019) 1270–1307.
34
35 668 doi:10.2174/0929867325666171229133259.
36
37
38
39 669 [16] M.D. Norris, Expression of multidrug transporter MRP4/ABCC4 is a marker of poor
40
41 670 prognosis in neuroblastoma and confers resistance to irinotecan in vitro, Mol.
42
43 671 Cancer Ther. 4 (2005) 547–553. doi:10.1158/1535-7163.mct-04-0161.
44
45
46
47 672 [17] S. Copsel, C. Garcia, F. Diez, M. Vermeulem, A. Baldi, L.G. Bianciotti, F.G.M. Russel,
48
49 673 C. Shayo, C. Davio, Multidrug resistance protein 4 (MRP4/ABCC4) regulates cAMP
50
51 674 cellular levels and controls human leukemia cell proliferation and differentiation, J.
52
53 675 Biol. Chem. 286 (2011) 6979–6988. doi:10.1074/jbc.M110.166868.
54
55
56
57 676 [18] A. Carozzo, A. Yaneff, N. Gomez, N. Di Siervi, A. Sahores, F. Diez, A.I. Attorresi, A.

677 Rodriguez-Gonzalez, F. Monczor, N. Fernandez, M. Abba, C. Shayo, C. Davio,
1
2 678 IDENTIFICATION OF MRP4/ABCC4 AS A TARGET FOR REDUCING THE
3
4 679 PROLIFERATION OF PANCREATIC DUCTAL ADENOCARCINOMA CELLS BY
5
6 680 MODULATING THE cAMP EFFLUX, Mol. Pharmacol. (2019) mol.118.115444.
7
8
9 681 doi:10.1124/mol.118.115444.
10
11 682 [19] T.J. Kochel, J.C. Reader, X. Ma, N. Kundu, A.M. Fulton, Multiple drug resistance-
12
13 683 associated protein (MRP4) exports prostaglandin E₂ (PGE₂) and contributes to
14
15 684 metastasis in basal/triple negative breast cancer, Oncotarget. 8 (2017) 6540–6554.
16
17 685 doi:10.18632/oncotarget.14145.
18
19
20 686 [20] L. Tirinato, F. Pagliari, T. Limongi, M. Marini, a. Falqui, J. Seco, P. Candeloro, C.
21
22 687 Liberale, E. Di Fabrizio, An Overview of Lipid Droplets in Cancer and Cancer Stem
23
24 688 Cells, Stem Cells Int. 2017 (2017). doi:10.1155/2017/1656053.
25
26
27 689 [21] K. Saito, E. Arai, K. Maekawa, M. Ishikawa, H. Fujimoto, R. Taguchi, K. Matsumoto,
28
29 690 Y. Kanai, Y. Saito, Lipidomic Signatures and Associated Transcriptomic Profiles of
30
31 691 Clear Cell Renal Cell Carcinoma, Sci. Rep. 6 (2016) 1–12. doi:10.1038/srep28932.
32
33
34 692 [22] J. Jones, H. Otu, D. Spentzos, S. Kolia, M. Inan, W.D. Beecken, C. Fellbaum, X. Gu,
35
36 693 M. Joseph, A.J. Pantuck, D. Jonas, T.A. Libermann, Gene signatures of progression
37
38 694 and metastasis in renal cell cancer, Clin. Cancer Res. 11 (2005) 5730–5739.
39
40 695 doi:10.1158/1078-0432.CCR-04-2225.
41
42
43 696 [23] T. Barrett, S.E. Wilhite, P. Ledoux, C. Evangelista, I.F. Kim, M. Tomashevsky, K. a.
44
45 697 Marshall, K.H. Phillippy, P.M. Sherman, M. Holko, A. Yefanov, H. Lee, N. Zhang, C.L.
46
47 698 Robertson, N. Serova, S. Davis, A. Soboleva, NCBI GEO: Archive for functional
48
49 699 genomics data sets - Update, Nucleic Acids Res. 41 (2013) 991–995.
50
51 700 doi:10.1093/nar/gks1193.
52
53
54
55
56
57
58
59
60
61
62
63
64
65

1
2
3
4
5
6
7
8
9
10
11
12
13
14
15
16
17
18
19
20
21
22
23
24
25
26
27
28
29
30
31
32
33
34
35
36
37
38
39
40
41
42
43
44
45
46
47
48
49
50
51
52
53
54
55
56
57
58
59
60
61
62
63
64
65

701 [24] T.R. Stoyanoff, J.P. Rodríguez, J.S. Todaro, J.D. Espada, J.P. Melana Colavita, N.C.
702 Brandan, A.M. Torres, M.V. Aguirre, Tumor biology of non-metastatic stages of
703 clear cell renal cell carcinoma; overexpression of stearyl desaturase-1, EPO/EPO-R
704 system and hypoxia-related proteins, *Tumor Biol.* (2016). doi:10.1007/s13277-016-
705 5279-4.

706 [25] A. Carozzo, F. Diez, N. Gomez, M. Cabrera, C. Shayo, C. Davio, N. Fernández, Dual
707 role of cAMP in the transcriptional regulation of Multidrug Resistance-Associated
708 Protein 4 (MRP4) in pancreatic adenocarcinoma cell lines, *PLoS One.* 10 (2015) 1–
709 13. doi:10.1371/journal.pone.0120651.

710 [26] J.M. Rubio, J.P. Rodríguez, L. Gil-de-Gómez, C. Guijas, M.A. Balboa, J. Balsinde,
711 Group V Secreted Phospholipase A 2 Is Upregulated by IL-4 in Human Macrophages
712 and Mediates Phagocytosis via Hydrolysis of Ethanolamine Phospholipids, *J.*
713 *Immunol.* 194 (2015) 3327–3339. doi:10.4049/jimmunol.1401026.

714 [27] L. Gil-de-Gómez, A.M. Astudillo, C. Guijas, V. Magrioti, G. Kokotos, M.A. Balboa, J.
715 Balsinde, Cytosolic Group IVA and Calcium-Independent Group VIA Phospholipase
716 A 2 s Act on Distinct Phospholipid Pools in Zymosan-Stimulated Mouse Peritoneal
717 Macrophages , *J. Immunol.* 192 (2014) 752–762. doi:10.4049/jimmunol.1302267.

718 [28] P. Lebrero, A.M. Astudillo, J.M. Rubio, L. Fernández-Caballero, G. Kokotos, M.A.
719 Balboa, J. Balsinde, Cellular Plasmalogen Content Does Not Influence Arachidonic
720 Acid Levels or Distribution in Macrophages: A Role for Cytosolic Phospholipase A2y
721 in Phospholipid Remodeling, *Cells.* 8 (2019) 799. doi:10.3390/cells8080799.

722 [29] R.A.M.H. van Aubel, P.H.E. Smeets, J.G.P. Peters, R.J.M. Bindels, F.G.M. Russel, The
723 MRP4/ABCC4 gene encodes a novel apical organic anion transporter in human
724 kidney proximal tubules: putative efflux pump for urinary cAMP and cGMP., *J. Am.*

1
2
3
4
5
6
7
8
9
10
11
12
13
14
15
16
17
18
19
20
21
22
23
24
25
26
27
28
29
30
31
32
33
34
35
36
37
38
39
40
41
42
43
44
45
46
47
48
49
50
51
52
53
54
55
56
57
58
59
60
61
62
63
64
65

725 Soc. Nephrol. 13 (2002) 595–603.

726 <http://www.ncbi.nlm.nih.gov/pubmed/11856762>.

727 [30] V. Buxhofer-Ausch, L. Secky, K. Wlcek, M. Svoboda, V. Kounnis, E. Briasoulis, A.G.
728 Tzakos, W. Jaeger, T. Thalhammer, Tumor-Specific Expression of Organic Anion-
729 Transporting Polypeptides: Transporters as Novel Targets for Cancer Therapy, J.
730 Drug Deliv. 2013 (2013) 1–12. doi:10.1155/2013/863539.

731 [31] N. Glube, A. Giessl, U. Wolfrum, P. Langguth, Caki-1 cells represent an in vitro
732 model system for studying the human proximal tubule epithelium, Nephron - Exp.
733 Nephrol. 107 (2007). doi:10.1159/000107804.

734 [32] L. Peng, Y. Hu, D. Chen, S. Jiao, S. Sun, Ubiquitin specific peptidase 21 regulates
735 interleukin-8 expression, stem-cell like property of human renal cell carcinoma,
736 Oncotarget. 7 (2016) 42007–42016. doi:10.18632/oncotarget.9751.

737 [33] C. Guijas, J.P. Rodríguez, J.M. Rubio, M.A. Balboa, J. Balsinde, Phospholipase A2
738 regulation of lipid droplet formation, Biochim. Biophys. Acta - Mol. Cell Biol. Lipids.
739 1841 (2014) 1661–1671. doi:10.1016/j.bbalip.2014.10.004.

740 [34] E.E. Spangenburg, S.J.P. Pratt, L.M. Wohlers, R.M. Lovering, Use of BODIPY
741 (493/503) to Visualize Intramuscular Lipid Droplets in Skeletal Muscle, J. Biomed.
742 Biotechnol. 2011 (2011) 1–8. doi:10.1155/2011/598358.

743 [35] Y. Ohsaki, Y. Shinohara, M. Suzuki, T. Fujimoto, A pitfall in using BODIPY dyes to
744 label lipid droplets for fluorescence microscopy, Histochem. Cell Biol. 133 (2010)
745 477–480. doi:10.1007/s00418-010-0678-x.

746 [36] T. Chanmee, P. Ontong, K. Konno, N. Itano, Tumor-associated macrophages as
747 major players in the tumor microenvironment, Cancers (Basel). 6 (2014) 1670–
748 1690. doi:10.3390/cancers6031670.

- 1
2
3
4
5
6
7
8
9
10
11
12
13
14
15
16
17
18
19
20
21
22
23
24
25
26
27
28
29
30
31
32
33
34
35
36
37
38
39
40
41
42
43
44
45
46
47
48
49
50
51
52
53
54
55
56
57
58
59
60
61
62
63
64
65
- 749 [37] K.A. Khan, R.S. Kerbel, Improving immunotherapy outcomes with anti-angiogenic
750 treatments and vice versa, *Nat. Rev. Clin. Oncol.* 15 (2018) 310–324.
751 doi:10.1038/nrclinonc.2018.9.
- 752 [38] D. Wu, P. Yotnda, Induction and testing of hypoxia in cell culture, *J. Vis. Exp.* (2011)
753 2–5. doi:10.3791/2899.
- 754 [39] G. Jin, B. Liu, Z. You, T. Bambakidis, E. Dekker, J. Maxwell, I. Halaweish, D. Linzel,
755 H.B. Alam, A. Arbor, Development of a novel neuroprotective strategy: Combined
756 treatment with hypothermia and valproic acid improves survival in hypoxic
757 hippocampal cells, *Surgery.* 156 (2015) 221–228.
758 doi:10.1016/j.surg.2014.03.038.Development.
- 759 [40] P. Combe, E. De Guillebon, C. Thibault, C. Granier, E. Tartour, *Oncolimmunology*
760 Therapeutic vaccines in metastatic renal cell carcinoma, (2015) 37–41.
761 doi:10.1080/2162402X.2014.1001236.
- 762 [41] J. Li, M. Bauer, B. Moe, E.M. Leslie, X.F. Li, Multidrug Resistance Protein 4
763 (MRP4/ABCC4) Protects Cells from the Toxic Effects of Halobenzoquinones, *Chem.*
764 *Res. Toxicol.* 30 (2017) 1815–1822. doi:10.1021/acs.chemrestox.7b00156.
- 765 [42] Z. Zhang, J. Wang, B. Shen, C. Peng, M. Zheng, The ABCC4 gene is a promising
766 target for pancreatic cancer therapy, *Gene.* 491 (2012) 194–199.
767 doi:10.1016/j.gene.2011.09.029.
- 768 [43] M. Bagnoli, G.L. Beretta, L. Gatti, S. Pilotti, P. Alberti, E. Tarantino, M. Barbareschi,
769 S. Canevari, D. Mezzanzanica, P. Perego, Clinicopathological impact of
770 ABCC1/MRP1 and ABCC4/MRP4 in epithelial ovarian carcinoma., *Biomed Res. Int.*
771 2013 (2013) 143202. doi:10.1155/2013/143202.
- 772 [44] Y. Sun, N. Shi, H. Lu, J. Zhang, Y. Ma, Y. Qiao, Y. Mao, K. Jia, L. Han, F. Liu, H. Li, Z.

- 773 Lin, X. Li, X. Zhao, *ABCC4* copy number variation is associated with susceptibility to
774 esophageal squamous cell carcinoma, *Carcinogenesis*. 35 (2014) 1941–1950.
775 doi:10.1093/carcin/bgu043.
- 776 [45] Z. Wang, Y. Xu, X. Meng, F. Watari, H. Liu, X. Chen, Suppression of c-Myc is involved
777 in multi-walled carbon nanotubes' down-regulation of ATP-binding cassette
778 transporters in human colon adenocarcinoma cells, *Toxicol. Appl. Pharmacol.* 282
779 (2015) 42–51. doi:10.1016/j.taap.2014.11.002.
- 780 [46] V.R. Holla, M.G. Backlund, P. Yang, R. a. Newman, R.N. DuBois, Regulation of
781 prostaglandin transporters in colorectal neoplasia, *Cancer Prev. Res.* 1 (2008) 93–
782 99. doi:10.1158/1940-6207.CAPR-07-0009.
- 783 [47] M. Montani, T. Herrmanns, M. Müntener, P. Wild, T. Sulser, G. Kristiansen,
784 Multidrug resistance protein 4 (MRP4) expression in prostate cancer is associated
785 with androgen signaling and decreases with tumor progression, *Virchows Arch.* 462
786 (2013) 437–443. doi:10.1007/s00428-013-1390-8.
- 787 [48] K.M. Morrissey, S.L. Stocker, M.B. Wittwer, L. Xu, K.M. Giacomini, Renal
788 Transporters in Drug Development, *Annu. Rev. Pharmacol. Toxicol.* 53 (2013) 503–
789 529. doi:10.1146/annurev-pharmtox-011112-140317.
- 790 [49] B. Prasad, K. Johnson, S. Billington, C. Lee, G.W. Chung, C.D.A. Brown, E.J. Kelly, J.
791 Himmelfarb, J.D. Unadkat, Abundance of drug transporters in the human kidney
792 cortex as quantified by quantitative targeted proteomics, *Drug Metab. Dispos.* 44
793 (2016) 1920–1924. doi:10.1124/dmd.116.072066.
- 794 [50] F. Lin, Z. He, B. Hu, L. Tang, S. Zheng, Y. Sun, Z. Sheng, Y. Yao, The overexpression of
795 MRP4 is related to multidrug resistance in osteosarcoma cells, *J. Cancer Res. Ther.*
796 11 (2015) 18. doi:10.4103/0973-1482.143334.

- 1
2
3
4
5
6
7
8
9
10
11
12
13
14
15
16
17
18
19
20
21
22
23
24
25
26
27
28
29
30
31
32
33
34
35
36
37
38
39
40
41
42
43
44
45
46
47
48
49
50
51
52
53
54
55
56
57
58
59
60
61
62
63
64
65
- 797 [51] L. Oevermann, J. Scheitz, K. Starke, K. Köck, T. Kiefer, G. Dölken, J. Nießen, A.
798 Greinacher, W. Siegmund, M. Zygmunt, H.K. Kroemer, G. Jedlitschky, C. a. Ritter,
799 Hematopoietic stem cell differentiation affects expression and function of MRP4
800 (ABCC4), a transport protein for signaling molecules and drugs, *Int. J. Cancer*. 124
801 (2009) 2303–2311. doi:10.1002/ijc.24207.
- 802 [52] X. Zhang, L. Zhao, X. Li, X. Wang, L. Li, X. Fu, Z. Sun, Z. Li, F. Nan, Y. Chang, M. Zhang,
803 ATP-binding cassette sub-family C member 4 (ABCC4) is overexpressed in human
804 NK/T-cell lymphoma and regulates chemotherapy sensitivity: Potential as a
805 functional therapeutic target, *Leuk. Res.* 39 (2015) 1448–1454.
806 doi:10.1016/j.leukres.2015.10.001.
- 807 [53] D.J. Grignon, M. Che, Clear cell renal cell carcinoma, *Clin. Lab. Med.* 25 (2005) 305–
808 316. doi:10.1016/j.cll.2005.01.012.
- 809 [54] A. Myszczyzyn, A.M. Czarnecka, D. Matak, L. Szymanski, F. Lian, A. Kornakiewicz, E.
810 Bartnik, W. Kukwa, C. Kieda, C. Szczylik, The Role of Hypoxia and Cancer Stem Cells
811 in Renal Cell Carcinoma Pathogenesis, *Stem Cell Rev. Reports*. 11 (2015) 919–943.
812 doi:10.1007/s12015-015-9611-y.
- 813 [55] N. Mice, J.M. Fogh, T. Orfeo, One Hundred and Twenty-Seven Cultured Human
814 Tumor Cell Lines Producing Tumors in, *J Natl Cancer*. 59 (1977) 221–226.
- 815 [56] S.-J. Lee, J. Zhang, A.M.K. Choi, H.P. Kim, Mitochondrial Dysfunction Induces
816 Formation of Lipid Droplets as a Generalized Response to Stress, *Oxid. Med. Cell.*
817 *Longev.* 2013 (2013) 1–10. doi:10.1155/2013/327167.
- 818 [57] M. Paar, C. Jüngst, N.A. Steiner, C. Magnes, F. Sinner, D. Kolb, A. Lass, R.
819 Zimmermann, A. Zumbusch, S.D. Kohlwein, H. Wolinski, Remodeling of lipid
820 droplets during lipolysis and growth in adipocytes, *J. Biol. Chem.* 287 (2012) 11164–

821 11173. doi:10.1074/jbc.M111.316794.

1
2 822 [58] A.M. Fajardo, G.A. Piazza, H.N. Tinsley, The role of cyclic nucleotide signaling
3
4 823 pathways in cancer: Targets for prevention and treatment, *Cancers (Basel)*. 6
5
6 824 (2014) 436–458. doi:10.3390/cancers6010436.

7
8
9 825 [59] C. Shayo, B.L. Legnazzi, F. Monczor, N. Fernández, M.E. Riveiro, A. Baldi, C. Davio,
10
11 826 The time-course of cyclic AMP signaling is critical for leukemia U-937 cell
12
13 827 differentiation, *Biochem. Biophys. Res. Commun.* 314 (2004) 798–804.
14
15 828 doi:10.1016/j.bbrc.2003.12.166.

16
17
18
19 829 [60] C.R. Santos, A. Schulze, Lipid metabolism in cancer, *FEBS J.* 279 (2012) 2610–2623.
20
21 830 doi:10.1111/j.1742-4658.2012.08644.x.

22
23
24
25 831

26 27 832 10. Legends

28
29
30 833 **Figure 1. Differential expression of MRP4 in tumors and normal samples. A.** *in-silico* analysis showing MRP4
31 834 over differentially expressed in Clear Cell Renal Carcinoma (ccRCC) samples when compared to their proper
32 835 non-tumoral samples (n=69). In opposition OATP4C1 is downregulated. The probe's ID for MRP4 and
33 836 OATP4C1 are shown in both cases. *Student's t-test* was used to determine differences. **** indicate
34 837 statistical significance at the p<0.0001 level. **B.** MRP4 mRNA was quantified by RT-qPCR, normalized by β -
35 838 actin mRNA and expressed relative to normal in tumor (Core or Periphery; n= 18). MRP4 is overexpressed in
36 839 most of the protein homogenates obtained from ccRCC (Core or Periphery) compared to distal normal renal
37 840 samples from the same patient. One patient was selected for illustration. Differences among groups were
38 841 analyzed by one-way analysis of variance (ANOVA; **** p<0.0001; *** p<0.001; * p<0.05). Densitometric
39 842 analysis of immunoreactive MRP4 band intensities (in arbitrary units) were normalized with those of β -actin.
40 843 **C – J.** Two representative patients of the analyzed samples were selected for immunohistochemical staining
41 844 for membranous MRP4 expression in ccRCC samples. **C & F.** In normal renal tissue, a full absence of glomerular
42 845 protein expression is observed in opposition to the highly ordered and polarized proximal tubular expression.
43 846 **D & G.** The expression of MRP4 in the tumor Core appears disordered with foci of intense expression. **E & H.**
44 847 In contrast peripheral tumor tissues show a weak reduction of MRP4 with infrequent intense pockets of
45 848 protein expression. **I.** Normal positive control of MRP4 expression in Colon. **J.** Semi-quantification of MRP4
46 849 expression and localization in ccRCC. Magnification 400x.

47 850
48 851
49 852 **Figure 2. MRP4 expression in renal cell lines. A.** MRP4 mRNA was quantified by RT-qPCR in Caki-1 and Caki-
50 853 2 cell lines. The MRP4 expression was normalized by β -actin mRNA. HCT-116 cell line was used as positive
51 854 control. Differences among groups were analyzed by one-way analysis of variance (ANOVA; * p<0.05). **B.**
52 855 Western blot analysis showing the protein expression in cell lines. **C.** Densitometric analysis of
53 856 immunoreactive MRP4 band intensities in renal cell lines. *Student's t-test* was used to determine differences.
54 857 * indicate statistical significance at the p<0.05 level. **D-F.** ICC detection and localization of MRP4 in HCT-116
55 858 (D), Caki-1 (E), Caki-2 (F). Note the only membranous expression profile in colon cells (black arrows) compared
56 859 to the intense cytoplasmic expression of both Caki cells (light blue and red arrows). Magnification 400x.

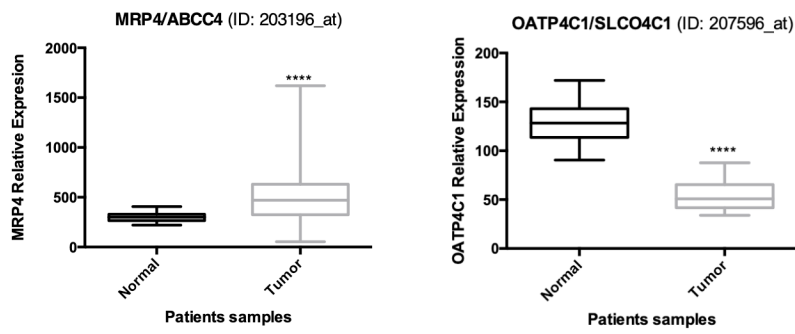
57 860
58 861 **Figure 3. cAMP efflux is mediated by MRP4 in Caki-1 and Caki-2 cells and it is engaged in cell
60 861 proliferation. A.** Cells were incubated with IBMX (1 mM) and subsequently stimulated with FSK (25 μ M) for
61
62
63
64
65

5 minutes. e-cAMP was measured in supernatants, whereas i-cAMP was obtained from cellular scrapings. **B.** Pharmacological inhibition of MRP4 with MK-571 (25 μ M) or Probenecid (0.5 mM) induced an accumulation of the cyclic nucleotide in the intracellular space in Caki-2 (light-blue). **C.** The role of MRP4 in cell proliferation was assayed in both Caki cell lines. Note that Caki-2 line has a shorter time of cellular duplication as demonstrated by XTT[®] proliferation assay. **D.** Cells monolayers were grown up to confluence and then were depleted of FBS-supplemented culture medium. Two hours later, different cAMP concentrations were added and cell proliferation was evaluated 48 h later. **E.** Cell cycle stages were evaluated using propidium iodide (PI) staining in flow cytometer. cAMP-treated cells showed a significant increase in Phase S.

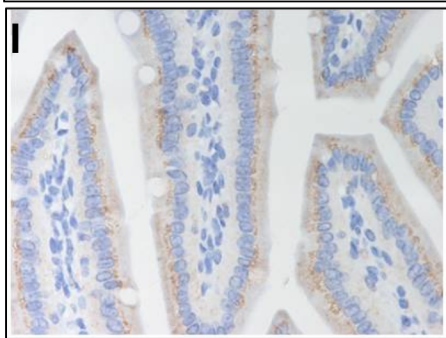
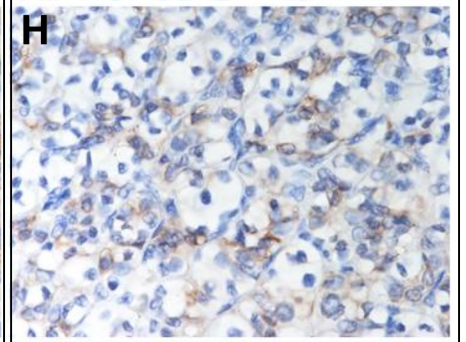
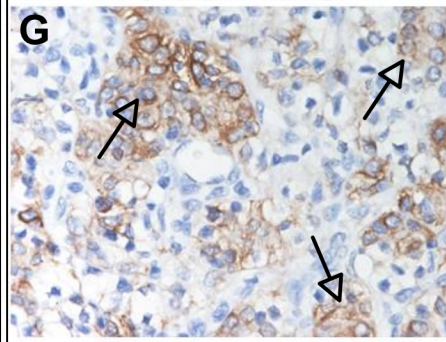
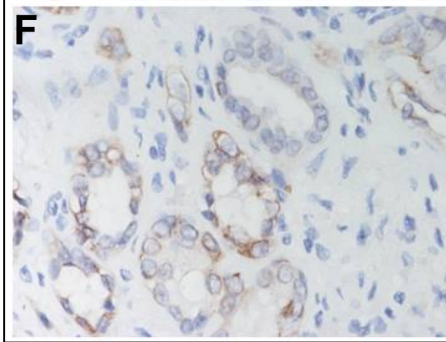
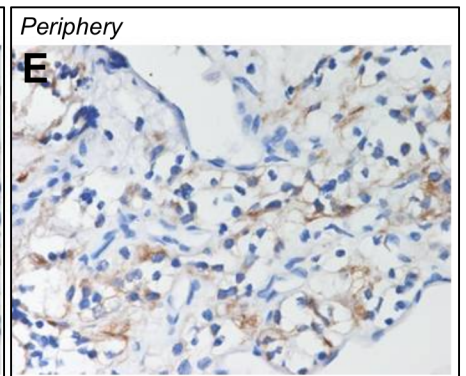
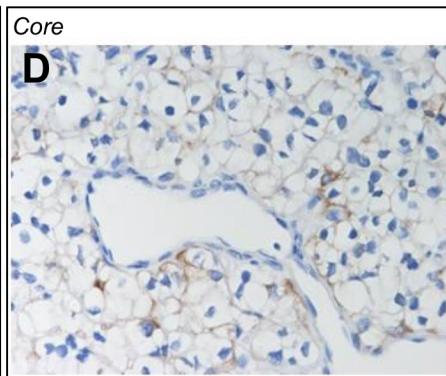
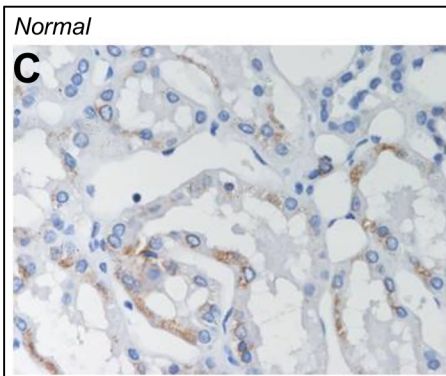
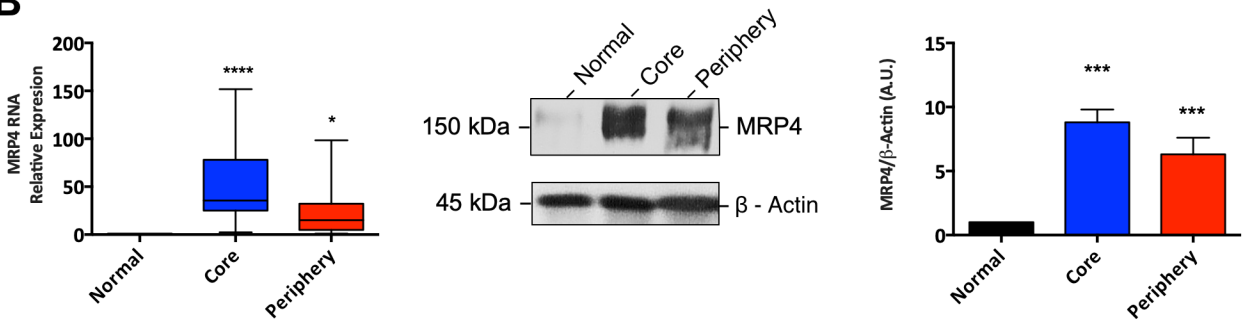
Figure 4. Pharmacological inhibition of MRP4 induced phenotypical changes, produced inhibition of cell proliferation and triggered apoptotic cell death. **A.** Gating strategy in control and treated cells. **B.** Caki-2 control cells (red) and treated with FSK + MK-571 (blue) for 18 h, and then they were stained with Bodipy[®] and acquired (2.10⁴ events) in linear mode. A shift to the right of the treated cells was observed, indicating an increase in cytoplasmic LD (cell stress signal). **C.** Media fluorescence intensity (MFI %) of the control and treated populations. **D.** Confocal microscopy of LD in Caki-2 controls. **E.** Positive control of LD biogenesis induced by OA (30 μ M). **F.** Caki-2 treated cells (MK-571 + FSK; both 25 μ M). Original magnification 400x. **G.** Total lipid extract of control and treated cells were obtained and the content of the TAG and CE fractions (LD) was analyzed by CG-MS. Fatty Acids (FA) esterified in cellular glycerol (TAG) and into cholesterol is shown. An elevation in FA content (particularly 16:0 and 18:0) is observed in cells treated with FSK + MK-571. **H.** Caki cells treated with FSK + MK-571 or FSK + Probenecid for 48 – 72 h exhibited an impaired cell proliferation. **I.** Cells treated with FSK + MK-571 (25 μ M) for 48 h showed a cellular accumulation in the Sub G₀ stage measured by staining with PI and evaluated by flow cytometry. **J.** Apoptosis cells death were studied analyzing caspase 3 activation by ICC. Cells exposed to FSK + MK-571 (both 25 μ M) by 48 h showed extensive deposition of caspase 3, similarly to those cells treated with staurosporin (STP; 1 μ M). Magnification 400x. Data are representative of three different experiments and are shown as mean \pm SD. Differences among groups were analyzed by ANOVA or *t*-student test correspondingly (* $p < 0.05$ or *** $p < 0.001$).

Figure 5. MRP4 is overexpressed under hypoxic conditions. **A.** Caki-2 cell viability in the range of 0-400 μ M CoCl₂ concentrations. Cell cytotoxicity was observed when cells were exposed to 400 μ M CoCl₂. **B.** Overexpression of HIF-2 α evaluated by qPCR under hypoxic conditions *in vitro*. **C-D.** ICC of HIF-2 α . Control cells show a weak and homogeneous cytoplasmic staining pattern of HIF-2 α ; in opposition, cell treated with 300 μ M CoCl₂ showed perinuclear or nuclear recruitment of the nuclear factor HIF-2 α (black arrows). Both panels **C** and **D** 100x magnification (lower right quadrants 400x). **E.** MRP4 mRNA expression measured by qPCR in normoxic and hypoxic conditions.

A



B



J

MRP4 Expression and localization in ccRCC

Tumor Section	+		++		+++		Total
	n	%	n	%	n	%	
Core	2	20%	4	40%	4	40%	10
Periphery	6	60%	4	40%	0	0	10

Figure 2

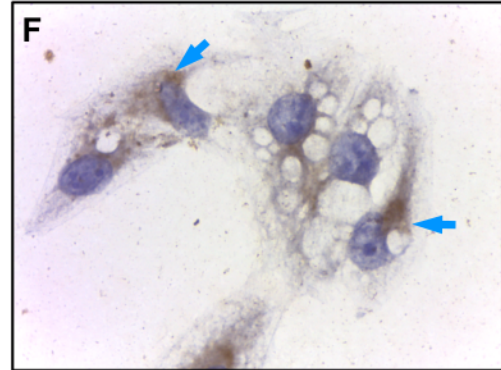
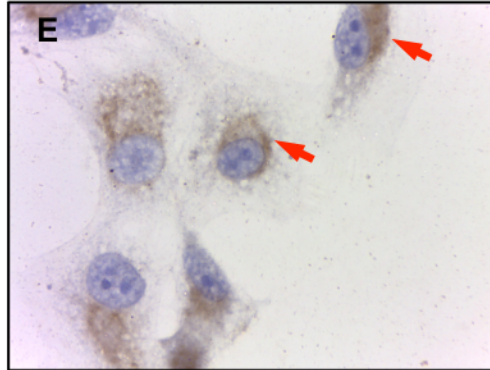
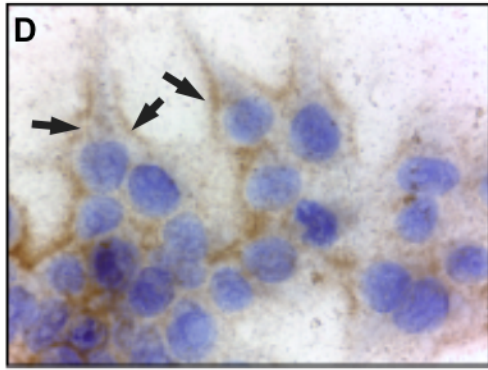
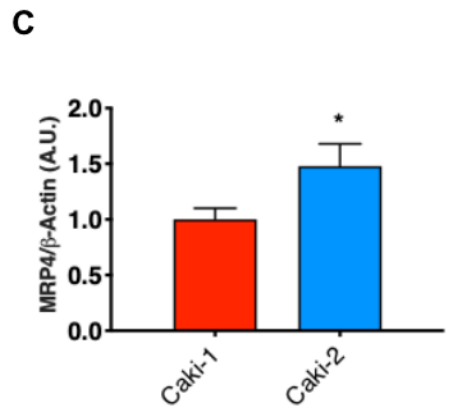
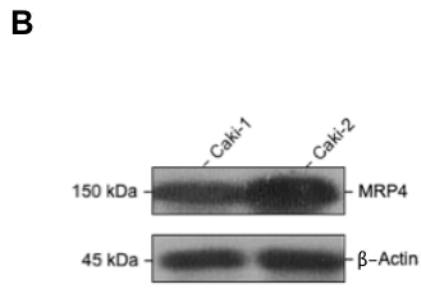
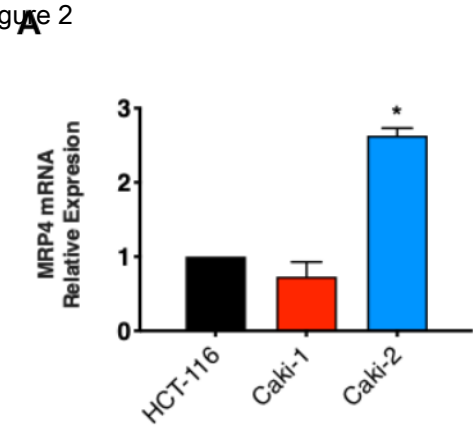
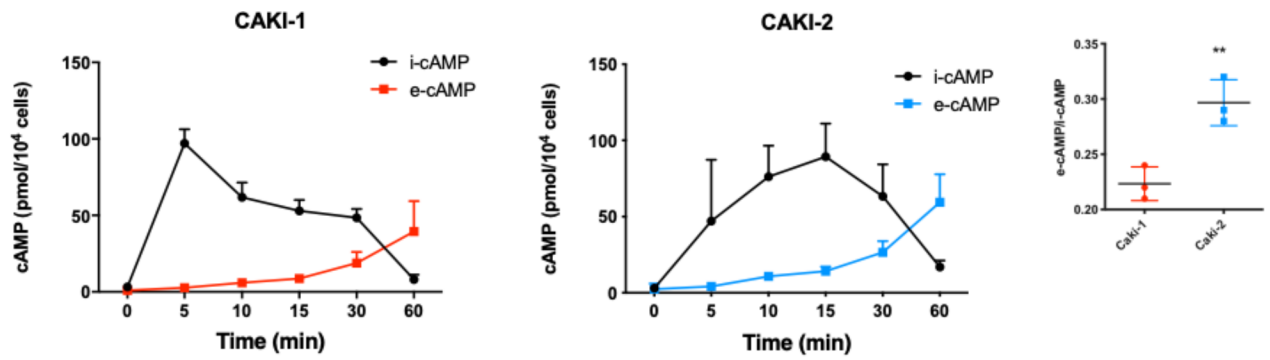
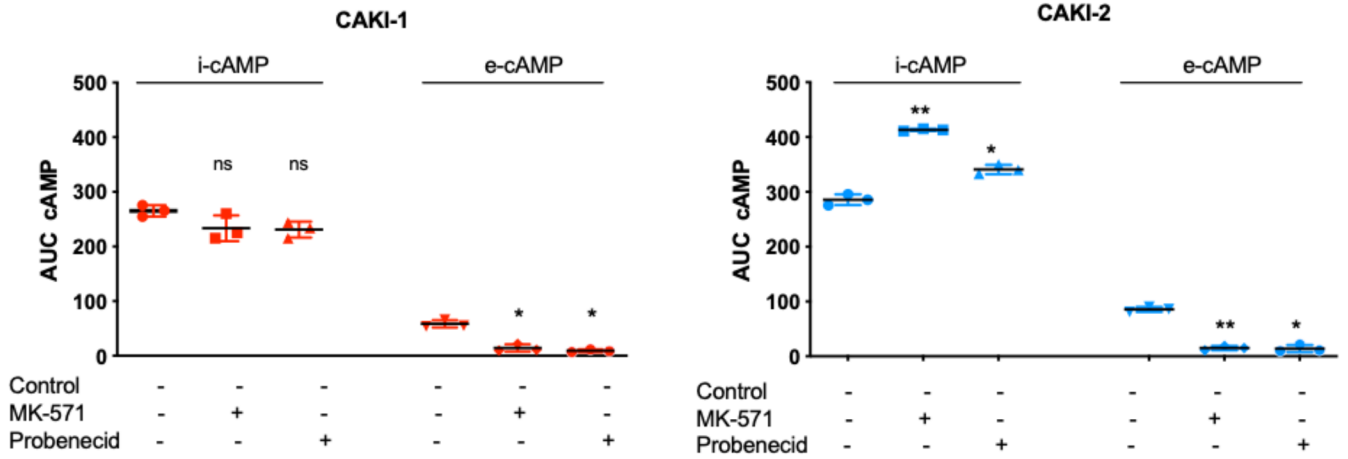


Figure 3

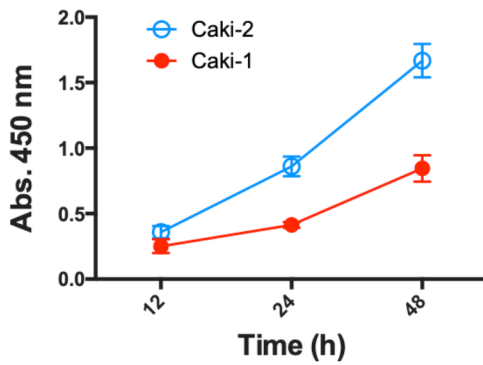
A



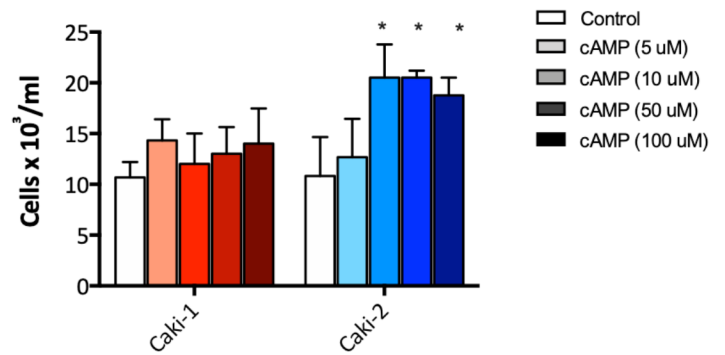
B



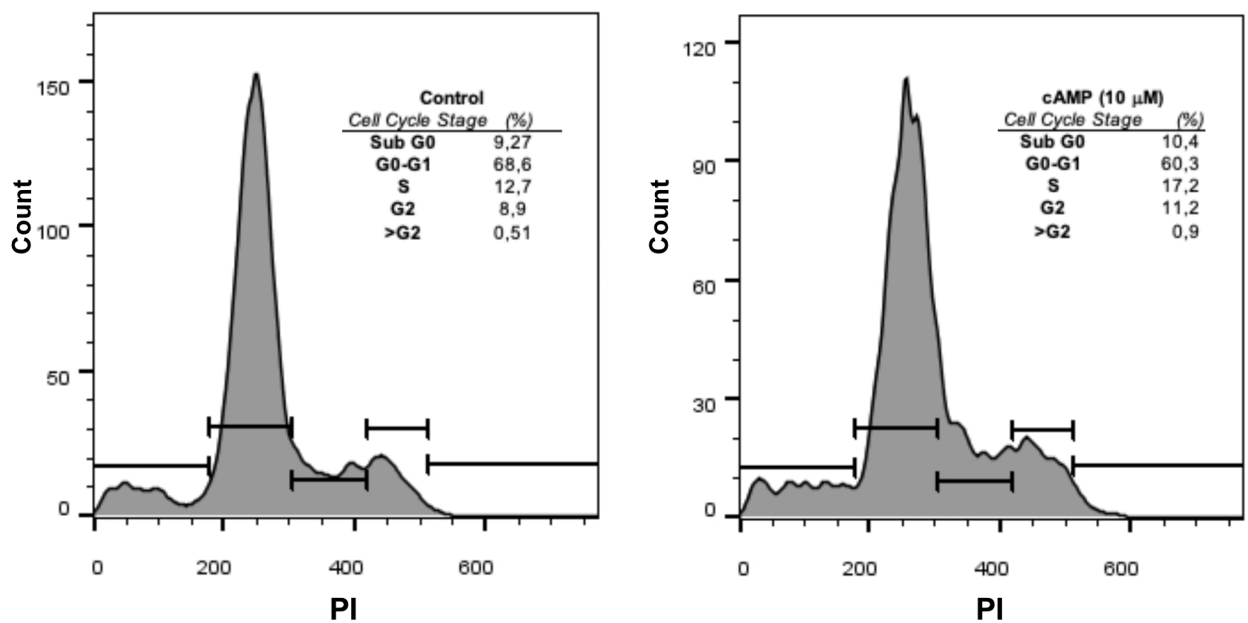
C



D



E



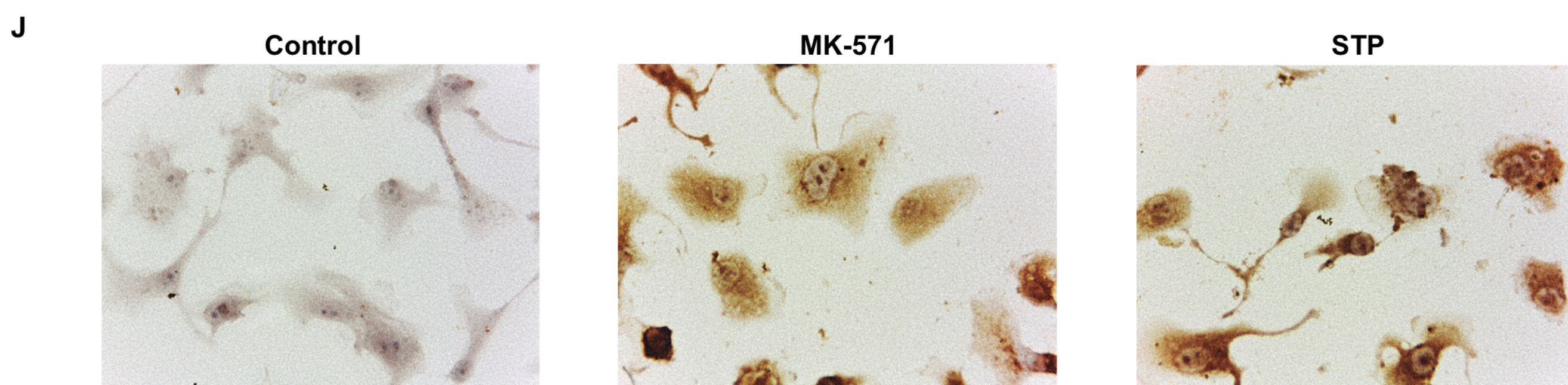
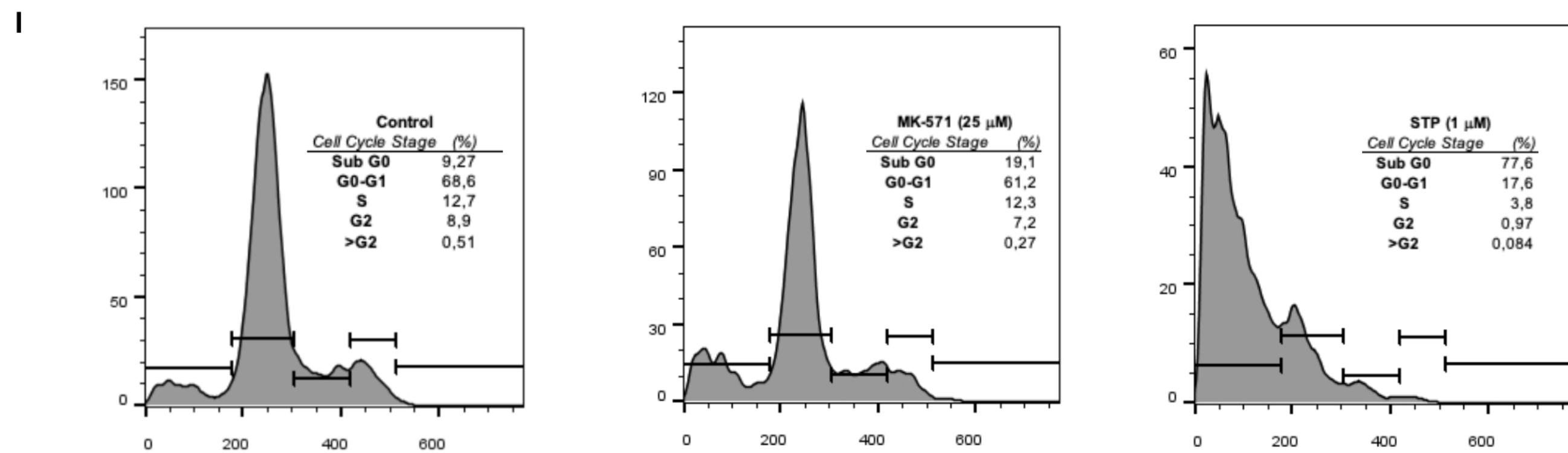
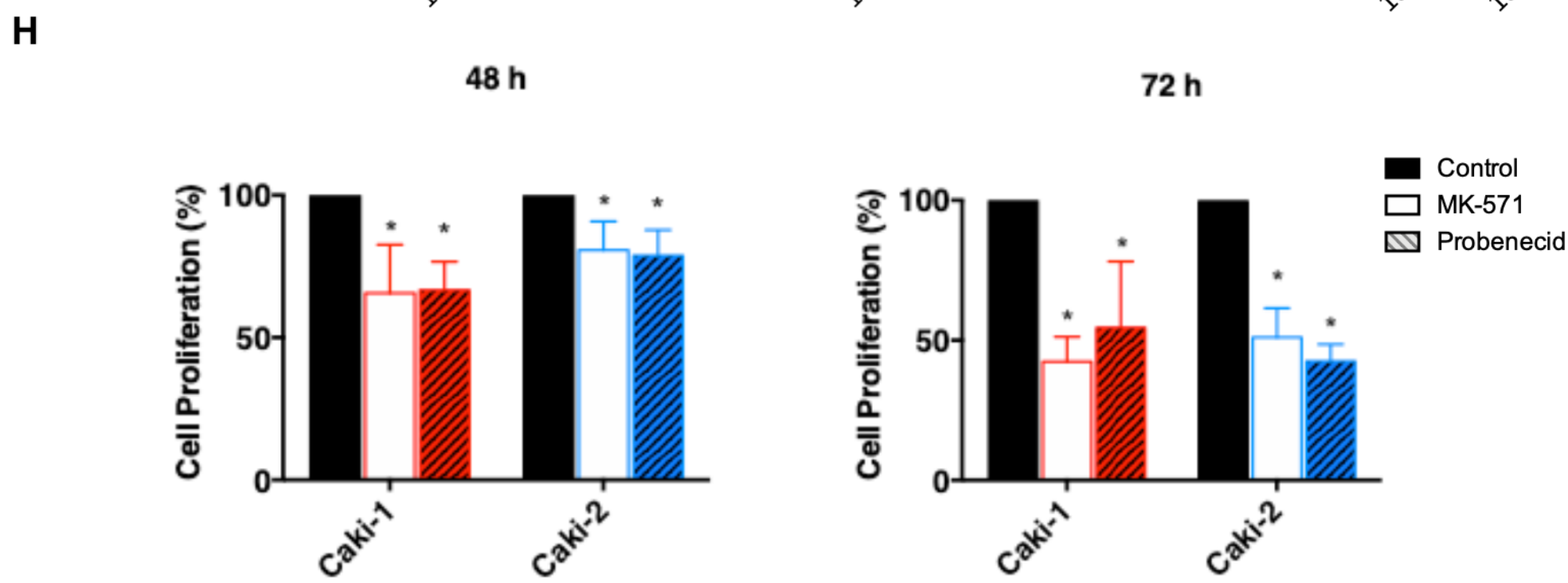
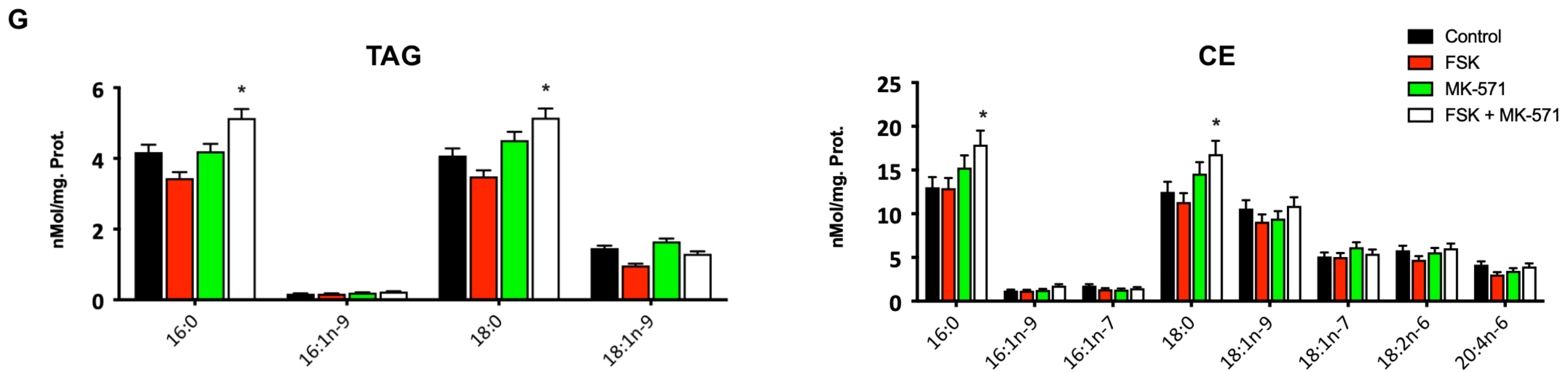
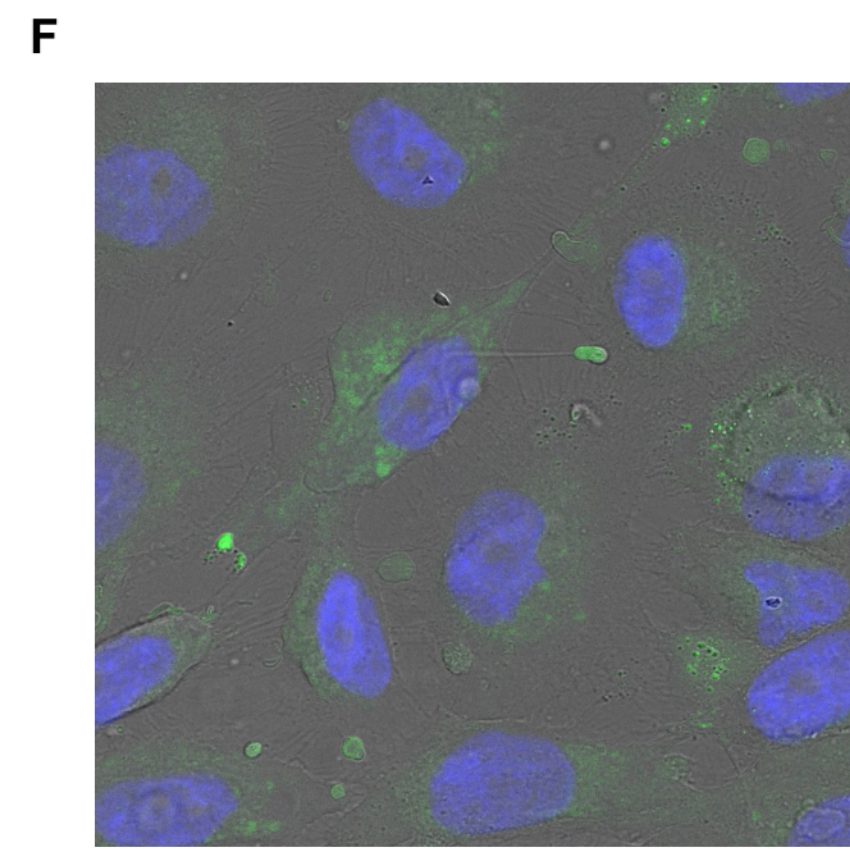
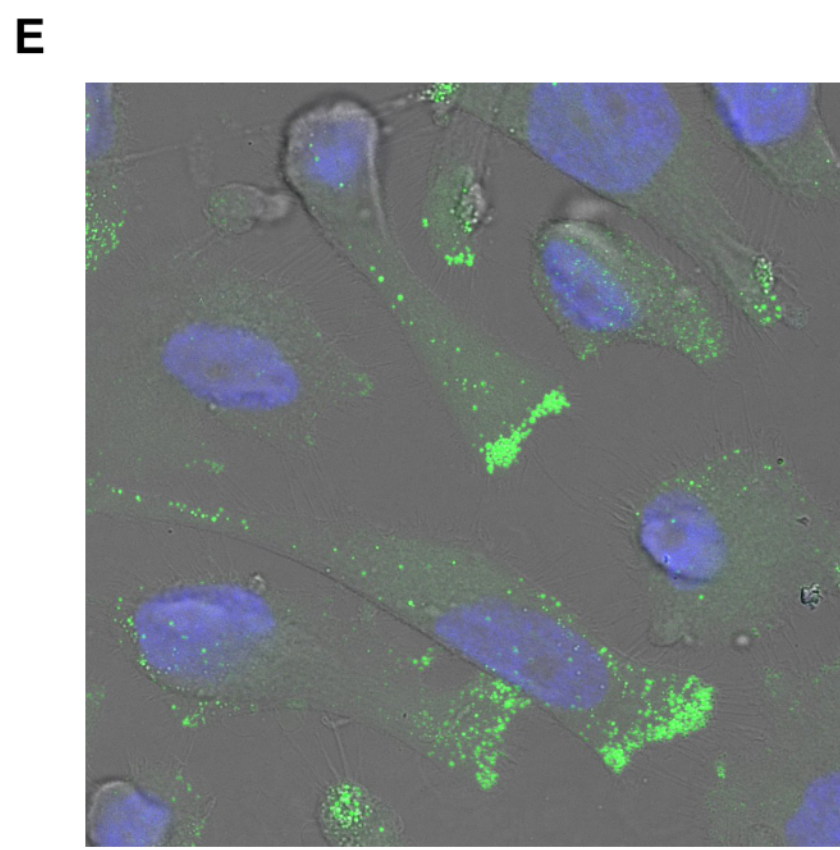
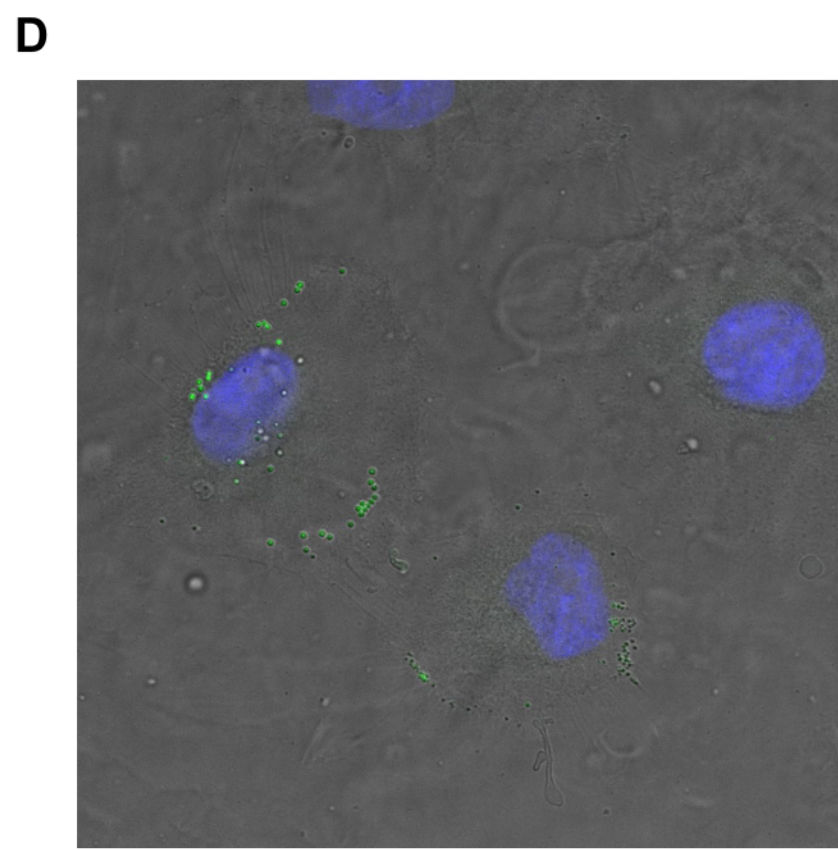
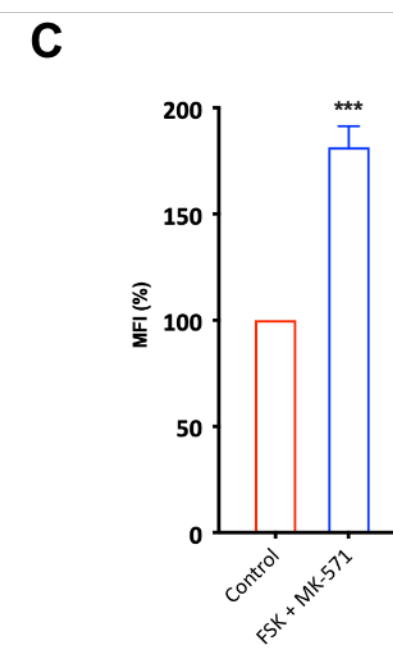
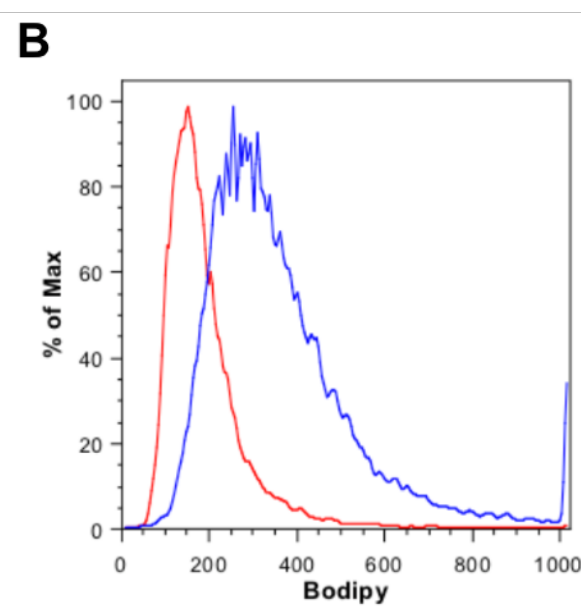
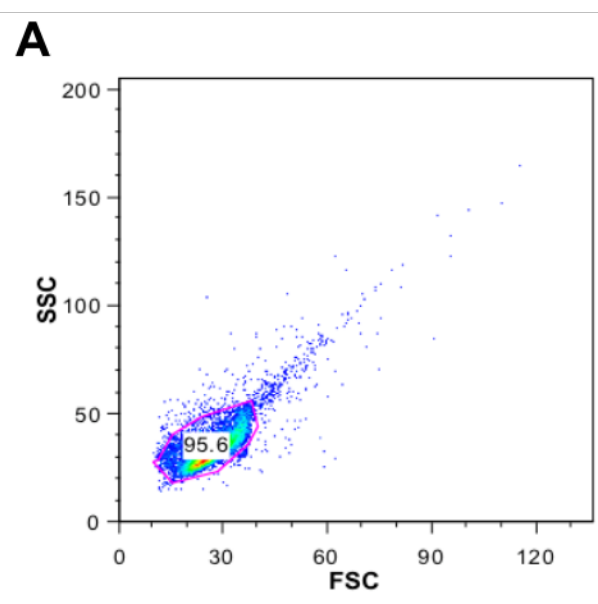
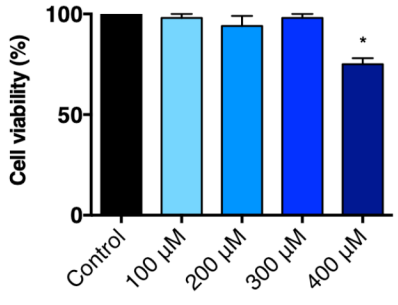
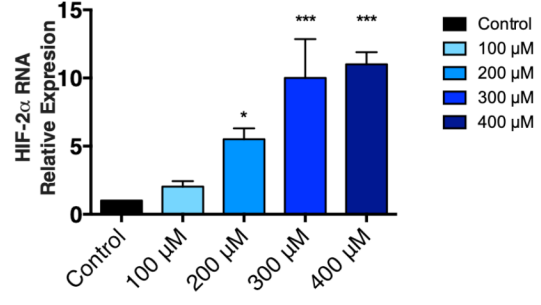


Figure 5

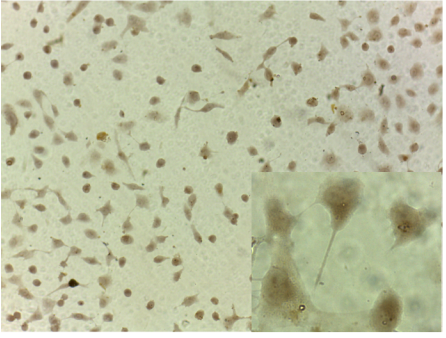
A



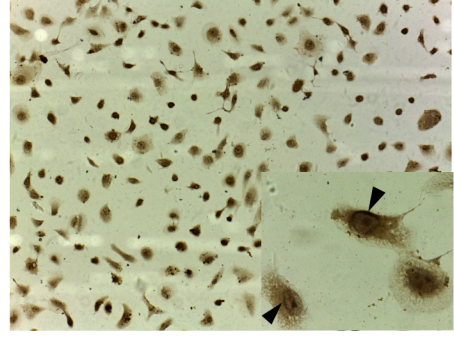
B



C



D



E

